Journal of Medicinal Chemistry



Article

# Discovery of 3-benzyl-1-(trans-4-((5-cyanopyridin-2-yl)amino)cyclohexyl)-1-arylurea derivatives as novel and selective cyclin-dependent kinase 12 (CDK12) inhibitors

Masahiro Ito, Toshio Tanaka, Akinori Toita, Noriko Uchiyama, Hironori Kokubo, Nao Morishita, Michael G Klein, Hua Zou, Morio Murakami, Mitsuyo Kondo, Tomoya Sameshima, Shinsuke Araki, Satoshi Endo, Tomohiro Kawamoto, Gregg B. Morin, Samuel A. Aparicio, Atsushi Nakanishi, Hironobu Maezaki, and Yasuhiro Imaeda

*J. Med. Chem.*, **Just Accepted Manuscript** • DOI: 10.1021/acs.jmedchem.8b00683 • Publication Date (Web): 01 Aug 2018



ACS Publications

is published by the American Chemical Society. 1155 Sixteenth Street N.W., Washington, DC 20036

# Discovery of 3-benzyl-1-(*trans*-4-((5-cyanopyridin-2-yl)amino)cyclohexyl)-1-arylurea derivatives as novel and selective cyclin-dependent kinase 12 (CDK12) inhibitors

*Masahiro Ito,*[*,†] *Toshio Tanaka,*[†,⊥] *Akinori Toita,*[†] *Noriko Uchiyama,*[†] *Hironori Kokubo,*[†,⊥] *Nao Morishita,*[†] *Michael G. Klein,*[‡] *Hua Zou,*[‡] *Morio Murakami,*[†] *Mitsuyo Kondo,*[†,⊥] *Tomoya Sameshima,*[†] *Shinsuke Araki,*[†] *Satoshi Endo,*[†,#] *Tomohiro Kawamoto,*[†,⊥] *Gregg B. Morin,*[§,@] *Samuel A. Aparicio,*[∥] *Atsushi Nakanishi,*[†] *Hironobu Maezaki,*[†,⊥] *and Yasuhiro Imaeda*[*,†]

[†]Pharmaceutical Research Division, Takeda Pharmaceutical Company Limited, 26-1, Muraoka-Higashi 2-chome, Fujisawa, Kanagawa 251-8555, Japan

[‡]Department of Structural Biology, Takeda California Inc., 10410 Science Center Dr., San Diego, CA 92121, United States

[§]Genome Sciences Centre, British Columbia Cancer Agency, 675 W. 10th Avenue, Vancouver, BC, V5Z 1L3, Canada

[@]Department of Medical Genetics, University of British Columbia, Vancouver, BC, V6H 3N1, Canada

[I]Department of Molecular Oncology, British Columbia Cancer Agency, 675 W. 10th Avenue, Vancouver, BC, V5Z 1L3, Canada

**Abstract:**

Cyclin-dependent kinase 12 (CDK12) plays a key role in the coordination of transcription with elongation and mRNA processing. CDK12 mutations found in tumors and CDK12 inhibition sensitize cancer cells to DNA-damaging reagents and DNA-repair inhibitors. This suggests that CDK12 inhibitors are potential therapeutics for cancer that may cause synthetic lethality. Here, we report the discovery of 3-benzyl-1-(*trans*-4-((5-cyanopyridin-2-yl)amino)cyclohexyl)-1-arylurea derivatives as novel and selective CDK12 inhibitors. Structure-activity relationship studies of a HTS hit, structure-based drug design, and conformation-oriented design using the Cambridge Structural Database afforded the optimized compound **2**, which exhibited not only potent CDK12 (and CDK13) inhibitory activity and excellent selectivity, but also good physicochemical properties. Furthermore, **2** inhibited the phosphorylation of Ser2 in the C-terminal domain of RNA polymerase II, and induced growth inhibition in SK-BR-3 cells. Therefore, **2** represents an excellent chemical probe for functional studies of CDK12 and could be a promising lead compound for drug discovery.

**Keywords:** Cyclin-dependent kinase 12 (CDK12), CDK12 inhibitor, RNA polymerase II (Pol II), C-terminal domain (CTD) of Pol II, conformation-oriented design, Cambridge Structural Database (CSD)

## Introduction

In eukaryotes, three distinct RNA polymerases (I–III) coordinate transcription: RNA polymerase I (Pol I) catalyzes the transcription of ribosomal RNA (rRNA) genes, RNA polymerase II (Pol II) is responsible for the transcription of protein-coding genes into messenger RNA (mRNA), and RNA polymerase III (Pol III) synthesizes small non-coding RNAs such as transfer RNAs (tRNAs). Pol II is the most studied of these RNA polymerases. It is well-established that the modulation of Pol II activity is regulated by the phosphorylation of a repeated motif (Y1-S2-P3-T4-S5-P6-S7) in the C terminal domain (CTD).[1] The number of Pol II CTD repeats vary from 26 in yeast to 52 in mammals, whereas this motif is completely absent in Pol I and Pol III. The number of CTD repeats tends to increase depending on the complexity of organisms. Truncation studies of Pol II CTD revealed a certain length of CTD repeats was necessary for yeast cell viability or mammalian cell growth.[2, 3] The main function of the CTD is to serve as a flexible binding scaffold for a variety of nuclear factors involved in the different phases of transcription. The regulation of the phosphorylation pattern on the CTD of Pol II helps to coordinate the assembly of complexes with transcription factors, chromatin modifiers, and RNA processing enzymes. Although phosphorylation of the CTD can occur on tyrosine, threonine, and serine residues,[4] phosphorylation at position 2 serines (Ser2) and position 5 serines (Ser5) are far more abundant than at other sites.[5] In general, Ser5 phosphorylation is essential for transcriptional initiation, whereas the phosphorylation of Ser2 contributes to transcriptional elongation and the recruitment of 3' RNA-processing factors, which play a major role in transcription termination. Five cyclin-dependent kinases (CDKs: 7, 8, 9, 12, and 13) are reported to phosphorylate the CTD of Pol II; thus, they are grouped together as “CTD kinases”.[1] All CTD kinases can phosphorylate Ser5, but only CDK9, CDK12, and CDK13 are responsible

for the phosphorylation of Ser2.[6–8] CDK12 and its close homolog CDK13 are unusually large proteins (1,490 and 1,512 amino acids, respectively, in humans) compared with other CDKs (e.g., CDK9, 372 amino acids).[9–13] Both CDK12 and CDK13 contain a central kinase domain and a N-terminal arginine-serine-rich (RS) domain,[14–16] which are frequently found in proteins involved in pre-mRNA splicing and RNA processing. As suggested by their structural features, CDK12 and CDK13 regulate co-transcriptional processing, including splicing and 3'-end RNA processing.[8,17–19] Recently, several differences between CDK12 and CDK13 were revealed by genetic depletion studies.[7] CDK12 is essential for the expression of longer genes with a high number of exons which are involved in DNA damage response pathway.[20,21] On the other hand, the loss of CDK13 does not affect the expression of such genes, but instead affect genes related to protein translation. Several mutations that affect the function of CDK12 have been identified in a variety of tumors. Consistent with the results of the genetic depletion experiments, these mutations in CDK12 make tumors sensitive to cytostatic DNA-damaging reagents, such as platinum analogs and alkylating agents, and the inhibitors of DNA-repair enzymes (PARP inhibitors).[22–24] This demonstrates the potential of CDK12 as a therapeutic target[25,26] that may induce synthetic lethality in cancers.[27]

In order to elucidate the detailed functions and biological roles of CDK12 and validate its potential as a therapeutic target, we initiated the exploration of molecular probes targeting CDK12. A high-throughput screen (HTS) of an in-house compound library was performed and hit compound **1** was identified as a modestly potent CDK12 inhibitor (Figure 1). Compound **1** showed optimal selectivity over other CTD kinases (CDK7, 8, and 9) and also showed potent inhibition of another CDK subtype, CDK2. As CDK2 is also known to regulate the cell cycle,[28] a significant reduction of the CDK2 inhibitory activity was necessary for the use of this chemical

series as molecular probes for CDK12 in cells. To improve the selectivity of **1** for CDK12 over CDK2, chemical optimization was conducted.

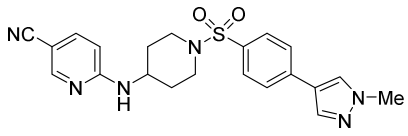

**1**

CDK12 $IC_{50}$ = 0.36 μM
CDK9 $IC_{50}$ > 30 μM
CDK8 $IC_{50}$ > 10 μM
CDK7 $IC_{50}$ > 10 μM
CDK2 $IC_{50}$ = 0.010 μM

**Figure 1**. Profile of hit compound **1** identified from in-house HTS campaign.

This report presents the discovery process of the structurally novel, potent, and selective non-covalent CDK12 inhibitor **2** by using a conformation-oriented design inspired by experimentally defined real conformations in the Cambridge Structural Database (CSD) [29,30] (Figure 2). In the process of our research, several selective CDK12 inhibitors **3** and **4** were reported by other groups.[31,32] As it is generally preferred to use structurally distinct chemical series for target validation to exclude the possibility of unknown off-target effects,[33,34] our novel compound **2** will provide another valuable option for molecular biologists and the pharmaceutical industry.

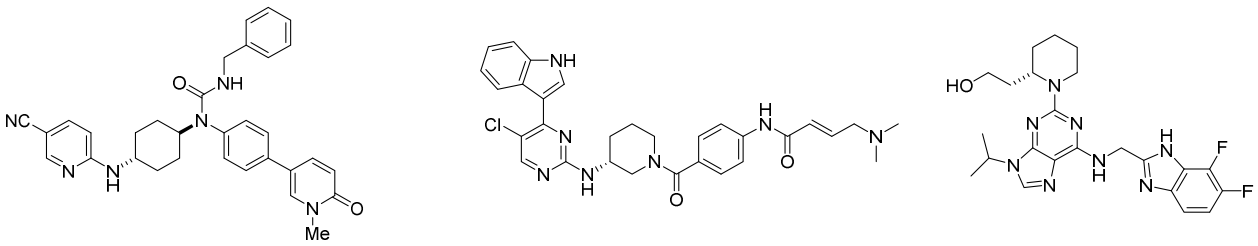

**2** **3** (THZ-531) **4**

**Figure 2**. Newly discovered selective CDK12 inhibitor **2** and reported inhibitors.

## Chemistry

The synthesis of compounds **1** and **7**–**13** is illustrated in Scheme 1. Commercially available 4-aminopiperidine derivative **5** was converted to intermediate **6** by sulfonylation, Suzuki coupling, and removal of the Boc group. Subsequent *N*-arylation of **6** under several conditions afforded target compounds **1** and **7**–**12**, whereas compound **13** was synthesized by *N*-methylation of **1**.

**Scheme 1.** Synthesis of **1** and **7**–**13**[a]

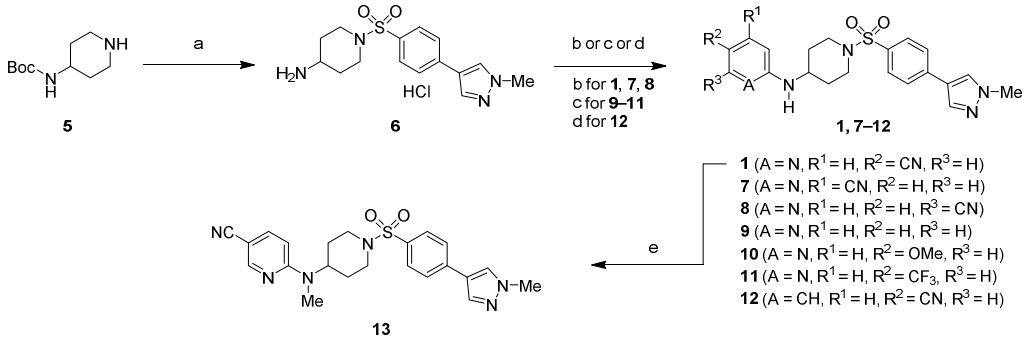


[a] Reagents and conditions: (a)(i) 4-bromobenzenesulfonyl chloride, $Et_3N$, THF, rt, 96%; (ii) 1-methyl-4-(4,4,5,5-tetramethyl-1,3,2-dioxaborolan-2-yl)-*1H*-pyrazole, $Pd(dppf)Cl_2 \cdot CH_2Cl_2$, $K_2CO_3$, DMF, $H_2O$, 100 °C, 83%; (iii) HCl/MeOH, rt, 99%.; (b) 6-fluoronicotinonitrile (for **1**) or 6-chloro-2-pyridinecarbonitrile (for **7**) or 2-chloroisonicotinonitrile (for **8**), DIPEA, NMP, 120–200 °C, 5–73%; (c) 2-bromopyridine (for **9**) or 2-bromo-5-methoxypyridine (for **10**) or 2-bromo-5-(trifluoromethyl)pyridine (for **11**), $Pd_2(dba)_3$, Davephos, *tert*-BuONa, toluene, 100 °C, 7–29%; (d) 4-fluorobenzonitrile, $K_2CO_3$, DMSO, 120 °C, 9%; (e) MeI, NaH, THF, DMF, 0 °C to rt, 85%.

The synthesis of compounds **16** and **17** is depicted in Scheme 2. Coupling of **14** with 6-chloronicotinonitrile, followed by removal of Boc group, yielded intermediate **15**. Then, acylation of **15** using 4-bromobenzoyl chloride and subsequent Suzuki coupling afforded compound **16**. Alkylation of **15** using 4-bromobenzyl bromide, followed by Suzuki coupling, yielded compound **17**.

**Scheme 2.** Synthesis of **16** and **17**[a]

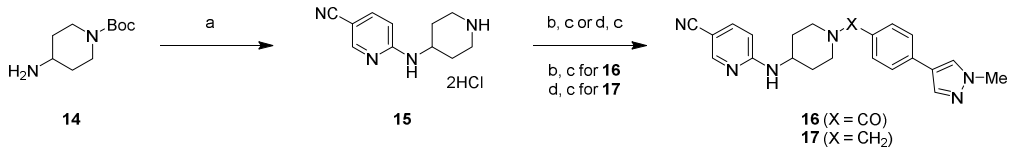


[a] Reagents and conditions: (a)(i) 6-chloronicotinonitrile, DIPEA, DMF, 120 °C, 66%; (ii) HCl/EtOAc, EtOH, rt, 98%; (b) 4-bromobenzoyl chloride, DIPEA, THF, rt, 89%; (c) 1-methyl-4-(4,4,5,5-tetramethyl-1,3,2-dioxaborolan-2-yl)-*1H*-pyrazole, $PdCl_2(Amphos)_2$,[35] $Cs_2CO_3$, DMF, 100 °C (microwave), 61–82%; (d) 4-bromobenzyl bromide, $K_2CO_3$, DMF, 80 °C, 96%.

Compounds **21**–**30**, **33**, and **34** were synthesized as shown in Scheme 3. Commercially available *trans*-1,4-cyclohexanediamine derivative **18** was converted to intermediate **20** using Buchwald-Hartwig coupling and Suzuki coupling sequentially. Amidation, methylsulfonylation, alkoxycarbonylation, or alkylaminocarbonylation of the arylamino group in **20**, followed by removal of the Boc group, and finally coupling with 2-halopyridine derivatives or 2-chloriquinazoline afforded compounds **21**–**29**. Compound **30** was obtained from **20** by deprotection of Boc group and coupling with 6-fluoronicotinonitrile. The *cis*-isomers **33** and **34** were synthesized from **31** in an analogous manner to those of **21** and **27**.

**Scheme 3.** Synthesis of **21**–**30**, **33**, and **34** [a]

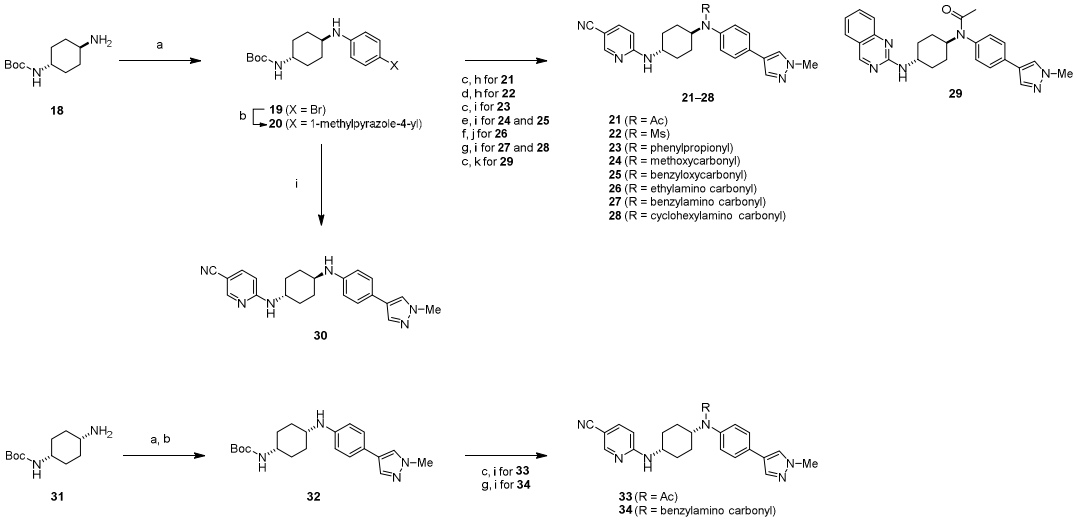


[a]Reagents and conditions: (a) 1-bromo-4-iodobenzene, *tert*-BuONa, $Pd_2(dba)_3$, Xantphos, toluene, 80 °C, 26–45%; (b) 1-methyl-4-(4,4,5,5-tetramethyl-1,3,2-dioxaborolan-2-yl)-*1H*-pyrazole, $Cs_2CO_3$, $PdCl_2(Amphos)_2$, DMF, $H_2O$, 100 °C, 84–96%;

(c) acetyl chloride (for **21**, **29**, and **33**) or phenylpropionyl chloride (for **23**), DIPEA, THF, 0 °C, 79–89%; (d) methanesulfonyl chloride, pyridine, rt, 81%; (e) methyl chloroformate (for **24**) or benzyl chloroformate (for **25**), DIPEA, $CH_2Cl_2$, rt, 62–85%; (f) ethyl isocyanate, THF, rt, 53%; (g) benzyl isocyanate (for **27** and **34**) or cyclohexylmethyl isocyanate (for **28**), THF, rt, 68–90%; (h) (i) TFA, rt (ii) 6-chloronicotinonitrile, DIPEA, DMF, 120 °C, 19–23%; (i) (i) HCl/EtOAc, rt (ii) 6-fluoronicotinonitrile, DIPEA, NMP, 80–100 °C, 33–82%; (j) (i) HCl/dioxane, $CH_2Cl_2$, rt (ii) 6-bromonicotinonitrile, $Cs_2CO_3$, DMF, rt, 15%; (k) (i) TFA, rt (ii) 2-chloroquinazoline, DBU, DMF, 120 °C, 37%.

Compounds **2**, **39**, **40**, **44**, **46**, and **47** were synthesized as depicted in Scheme 4. Intermediate **19** was converted to benzylurea **35** followed by reduction of the bromo group afforded **36**. Compound **37** was synthesized by Suzuki coupling of **35** and 3-pyridinylboronic acid. Compounds **35**–**37** were converted to aminopyridines **38**–**40**, respectively, by removal of the Boc group and subsequent coupling with 6-fluoronicotinonitrile. Suzuki coupling of bromide **38** with borates **41** and **42** yielded compounds **2** and **44**, respectively, whereas **38** was converted to borate **45** by Miyaura reaction followed by Suzuki coupling with 6- or 4-bromo-1-methylpyridin-2(1*H*)-one to give the designed compounds **46** and **47**.

**Scheme 4.** Synthesis of **2**, **39**, **40**, **44**, **46** and **47**[a]

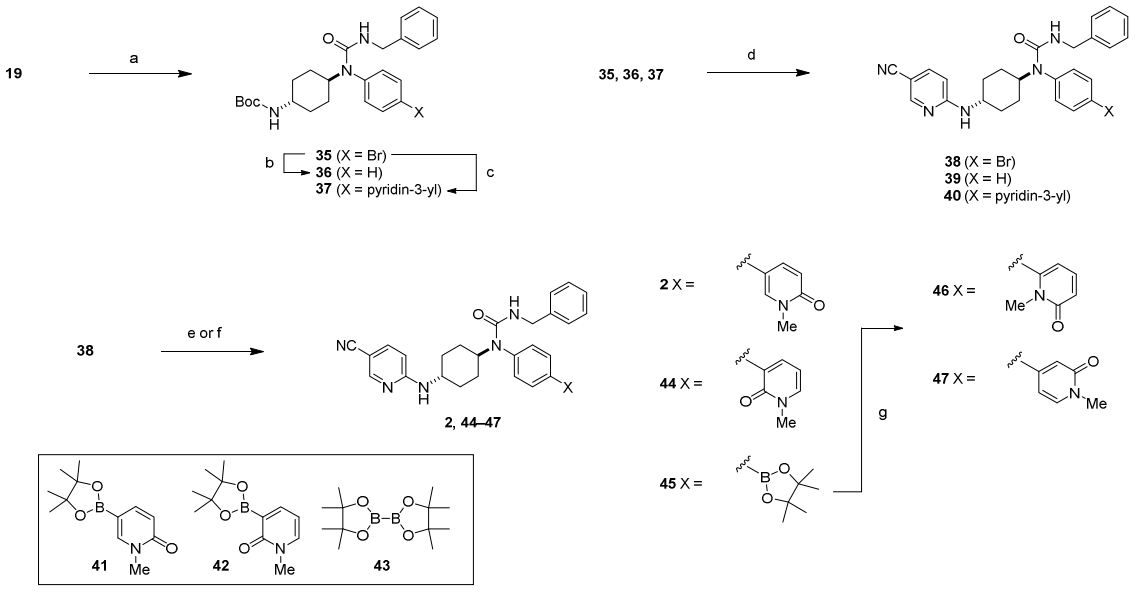

[a] Reagents and conditions: (a) benzyl isocyanate, $Et_3N$, THF, rt, 93%; (b) $H_2$, Pd/C, $Et_3N$, EtOH, THF, rt, quant.; (c) 3-pyridinylboronic acid, $Cs_2CO_3$, $PdCl_2(Amphos)_2$, DMF, $H_2O$, 100 °C, 95%; (d) (i) HCl/EtOAc, THF, rt (ii) 6-fluoronicotinonitrile, DIPEA, NMP, 100 °C, 53─80%; (e) **41** (for **2**), **42** (for **44**), AcOK, $Pd(dppf)Cl_2 \cdot CH_2Cl_2$, NMP, 80–100 °C, 35–69%; (f) **43**, AcOK, $Pd(dppf)Cl_2$, DMSO, 80 °C, 88%; (g) 6-bromo-1-methylpyridin-2(1*H*)-one (for **46**) or 4-bromo-1-methylpyridin-2(1*H*)-one (for **47**), $Cs_2CO_3$, $PdCl_2(Amphos)_2$, DMF, $H_2O$, 80 °C, 44–48%.

## Results & Discussion

Biological evaluation of CDK12, 13, and 9 inhibitory activity was conducted using the TR-FRET assay system (PerkinElmer), which detects the inhibition of the phosphorylation of an acceptor-labeled peptide substrate and reports the results as $IC_{50}$ values. The inhibitory activity of compounds against CDK7 and CDK8 was assessed by the binding assay using the TR-FRET assay system, in which an acceptor-labeled ligand was used as a probe against GST-tagged CDK7 or GST-tagged CDK8. The displacement of the probe was detected by the decrease in FRET signal, and the results were expressed as $IC_{50}$ values. The inhibitory activity of CDK2 was measured using a radiometric assay system with Histone H1 as the substrate and radiolabeled [$\gamma$-$^{33}$P] ATP. The radiolabeled substrate was detected and the results were expressed as $IC_{50}$ values.

The aminopyridyl moiety of the hit compound **1** is a prevalent substructure in hinge binding scaffolds for kinase inhibitors.[36–38] Thus, we hypothesized that the 6-aminonicotinonitrile moiety in compound **1** could bind to the hinge region of CDK12 and first addressed the modification of this moiety (Table 1). The analogs of **1**, such as benzonitrile (**12**) and *N*-methylamino derivative (**13**), showed decreased activity, which indicates that the aminopyridyl moiety is essential for activity, thereby supporting our assumption. It was also revealed that the 3-cyano group of **1** is critical for activity (**1** vs **7**–**9**). Considering the results of

the methoxy (**10**) and trifluoromethyl (**11**) derivatives, an electron withdrawing functional group was suggested to be required at the 3-position of the pyridine ring.

**Table 1.** SAR around the amino pyridyl moiety

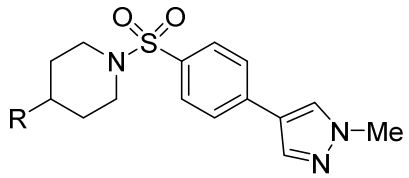


| Compound | R | CDK12 $IC_{50}$ (μM)[a] | CDK2 $IC_{50}$ (μM)[a] |
|---|---|---|---|
| **1** | 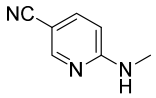 | 0.36 (0.18–0.69) | 0.01 (0.0088–0.012) |
| **12** | 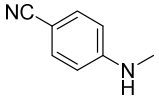 | >30 | NT |
| **13** | 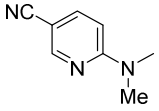 | >30 | 68 (15–322) |
| **7** | 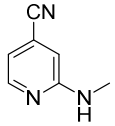 | >30 | 0.032 (0.028–0.036) |
| **8** | 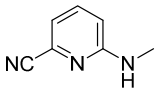 | >30 | 46 (32–66) |
| **9** | 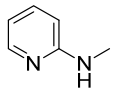 | >30 | 1.2 (0.97–1.4) |
| **10** | 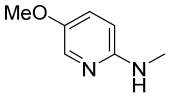 | >30 | 21 (17–26) |
| **11** | 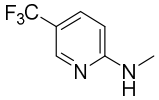 | 1.8 (0.87–3.7) | 0.0058 (0.0047–0.0071) |

[a] $n$ = 2, 95% confidence intervals shown in parentheses. NT = not tested.

To identify key structures to improve selectivity, preliminary docking models of compound **1** with CDK2 and CDK12 were constructed, respectively. From these, plausible models in which the aminopyridyl moiety interacts with the hinge region were selected (Figure 3). The

comparison of these models suggests that an oxygen atom from the sulfonyl moiety in **1** could interact with Lys89 of CDK2, while that interaction is not present in the model of CDK12 because the corresponding amino acid is not conserved in CDK12 and is replaced by Gly822. The assumption based on the model prompted us to modify the sulfonamide moiety to weaken or disrupt the putative interaction with Lys89 in CDK2.

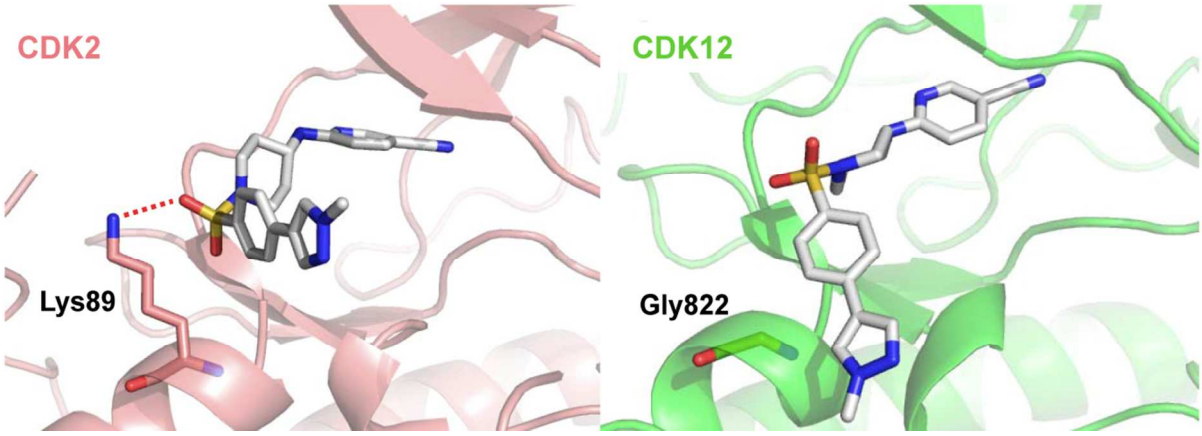


**Figure 3**. Docking models of compound **1** with CDK2 (left) and CDK12 (right). The sulfonamide moiety of **1** is suggested to interact with the side chain of Lys89 in CDK2. As the corresponding amino acid in CDK12 is Gly822, the hydrogen bonding could not be formed.

Replacement of the sulfonyl moiety in **1** with a carbonyl (**16**) or alkyl (**17**) moiety was not tolerated (Table 2). As sulfonamides are known to have strong conformational preferences in which the nitrogen lone pair bisects the O=S=O angle in the Newman projection (Figure 4, left),[28,39] we speculated that the biaryl moiety in **1** would be oriented perpendicularly against the piperidine ring. This notion was supported by the single crystal X-ray structure of **1** (Figure 4, right). Hence, it was inferred the orthogonal conformation of the sulfonamide should be mimicked to allow compounds to exhibit inhibitory activity. To explore the candidate substructures for the replacement of sulfonamide, we referred to the experimentally determined

conformations in the CSD.[40] The conformational search of the CSD suggested that *tert*-amides and *tert*-sulfonamides bearing a cyclohexyl moiety would show the desired conformation (Figure 5), in which the substituent on the amino moiety is perpendicular to the cyclohexyl ring. As the total number of useful examples in the CSD was too small to draw conclusions, we tested our speculation by direct experimentation. To that end, compounds **21**, **22**, and **33** were designed and synthesized (Figure 6 and Table 2). Although these replacements for sulfonamide are not common in medicinal chemistry, the *trans* isomers **21** and **22** exhibited similar levels of potency to compound **1**. In contrast, the decreased activity of the *cis* isomer **33** implies that the assumed di-equatorial conformation of the cyclohexyl ring in *trans* isomers might be necessary for the proper orientation of substituents (Supporting information 5, supplementary figures 5 and 10). Intriguingly, the selectivity of compounds **21** and **22** was better than that of **1** for CDK12 over CDK2. Especially **21** showed 3-fold selectivity for CDK12 over CDK2, whereas **22** still showed 3-fold stronger inhibitory activity for CDK2 rather than CDK12. This is probably attributable to the methylsulfonyl group of **22**, which might interact with Lys72 of CDK2 in a similar manner to the sulfonamide moiety of **1**. An overlay of the single crystal X-ray structures of **1**, **21**, and **22**, shown in Figure 7, revealed that these compounds adopt similar conformations, at least in their solid state. In contrast, the amide derivative **16** does not adopt the desired conformation. Contrary to **21** and **22**, the *trans*-cyclohexylamino derivative (**30**) resulted in reduced activity, which indicates that the acetyl group (**21**) or methylsulfonyl group (**22**) are essential for activity. The co-crystal structure of the analog of **21** (compound **29**)[41] with CDK12 was solved[42] (Figure 8). The resulting crystallographic model revealed the expected bioactive conformation described above. In addition, the oxygen atom of the acetyl group and the backbone of Asp819 are within hydrogen bonding distance. These observations indicate a dual role for the acetyl group,

comprising the adjustment of ligand conformation and formation of a hydrogen bonding with the protein.

**Table 2.** SAR of compounds **16**, **17**, **21**, **22**, **30**, and **33**

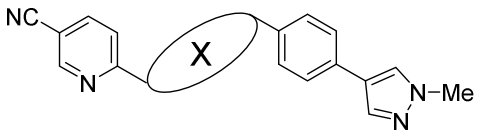


| Compound | X | CDK12 $IC_{50}$ (μM)[a] | CDK2 $IC_{50}$ (μM)[a] |
|---|---|---|---|
| **16** | 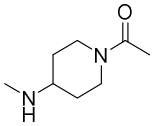 | 23 (18–28) | NT |
| **17** | 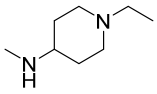 | 16 (14–19) | NT |
| **21** | 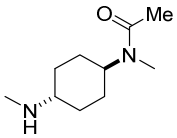 | 0.13 (0.090–0.18) | 0.47 (0.35–0.63) |
| **33** | 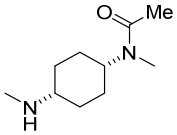 | >30 | >100 |
| **22** | 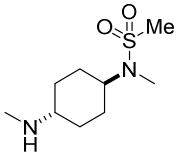 | 0.11 (0.083–0.15) | 0.031 (0.028–0.036) |
| **30** | 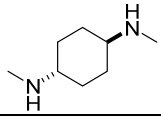 | 8.6 (4.9–15) | 9.8 (4.0–24) |

[a] $n$ = 2, 95% confidence intervals shown in parentheses. NT = not tested.

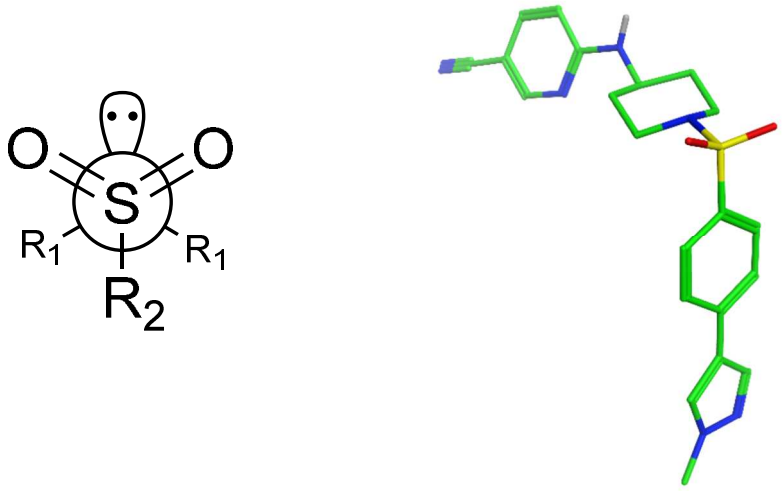


**Figure 4**. Preferences in the conformation of the sulfonamide moiety. Sulfonamides generally have strong conformational preferences, as shown in the Newman projection (left), which is preserved in the single crystal X-ray structure of **1** (right).

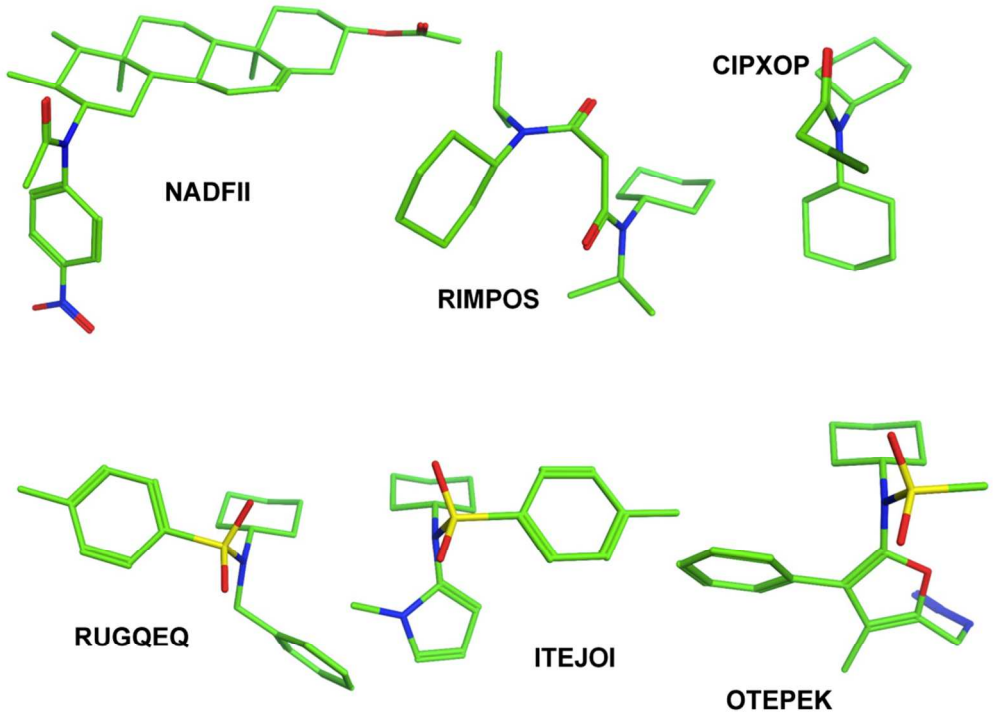


**Figure 5**. Representative examples of tertiary amides and tertiary sulfonamides bearing a cyclohexyl amino moiety in the Cambridge Structural Database.

.

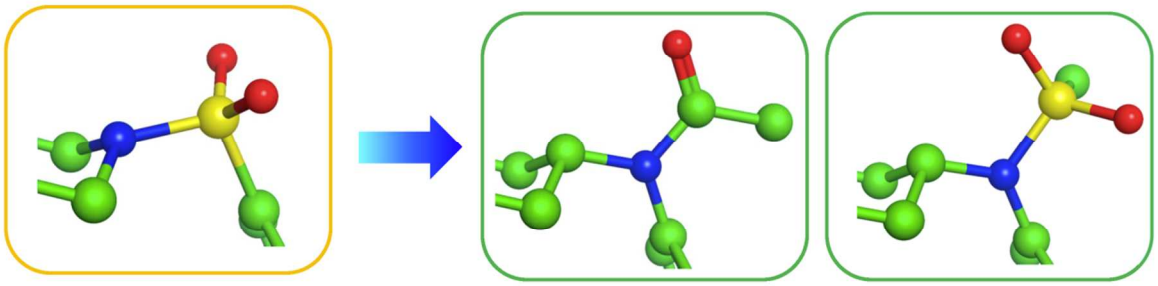

**Figure 6**. Schematic design of alternatives to the sulfonamide moiety. The designs are based on comparisons with experimentally determined conformations in the Cambridge Structural Database.

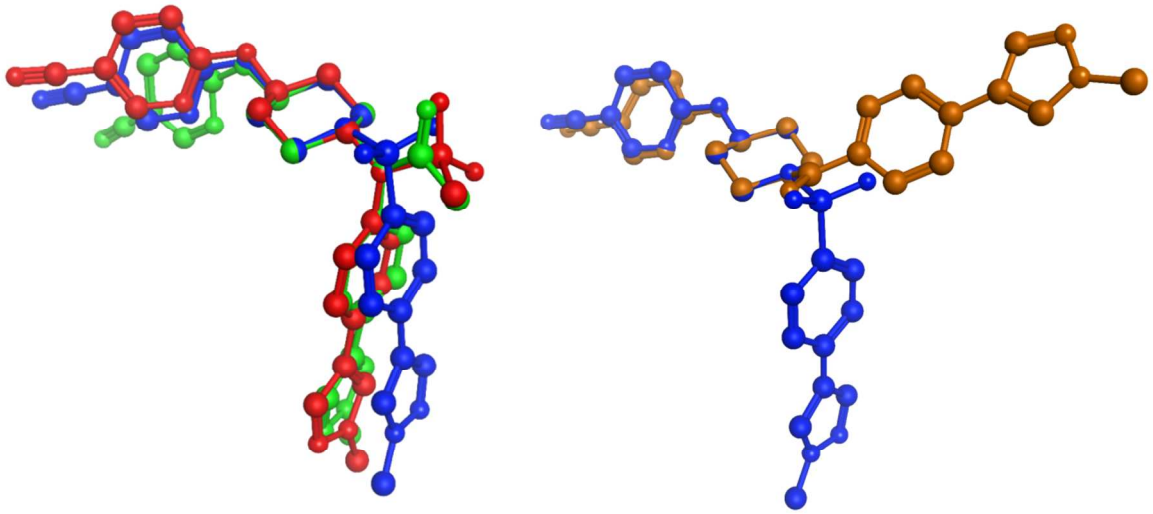

**Figure 7**. Overlay of single crystal X-ray structures of various ligands. Left: **1** (blue, CCDC 1835992), **21** (green, CCDC 1835994), and **22** (red, CCDC 1835995), with similar potencies,

overlap well with each other. Right: less potent **16** (amber, CCDC 1835993) exhibited a different conformation to **1** (blue).

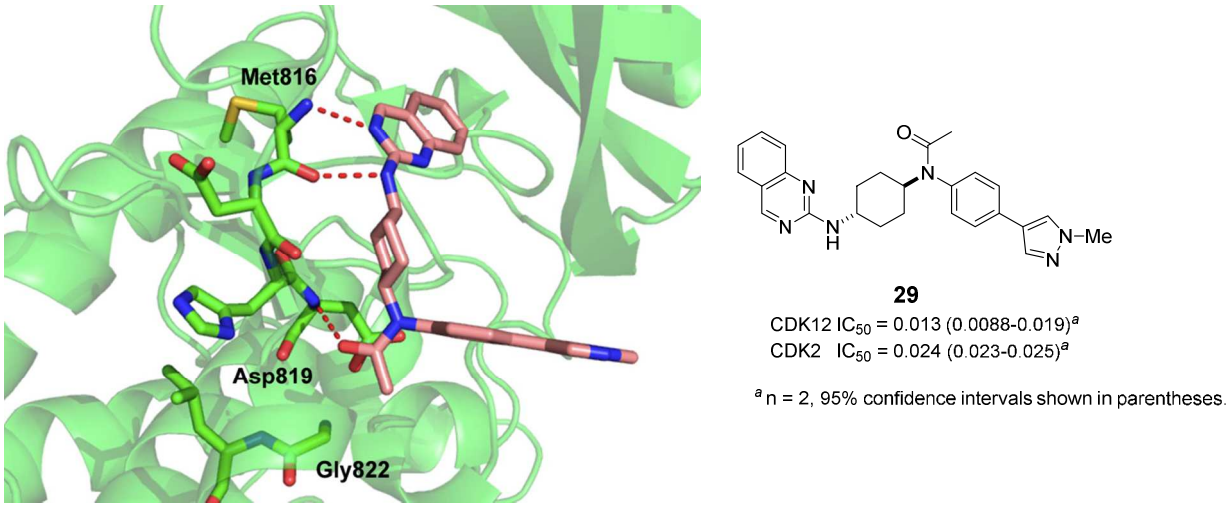


**Figure 8**. The X-ray co-crystal structure of **29** with CDK12 and cyclin K (PDB:6CKX, 2.75Å). Compound **29** occludes the ATP-binding site of CDK12 and the aminoquinazoline moiety interacts with Met816 in the hinge region. The carbonyl oxygen in the center of the compound is within hydrogen bonding distance of the backbone Asp819. The pyrazole moiety of **29** extends out towards the solvent.

Based on the in vitro results, further derivatization of compound **21** was conducted to identify more selective analogues. Replacement of the acetyl group with a variety of substituents was examined, and representative results are shown in Table 3. The methyl carbamate (**24**) and ethylurea derivatives (**26**) showed similar levels of CDK12 inhibitory activity, whereas the selectivity over CDK2 was slightly improved. Larger substituents, such as phenylpropanamide (**23**) and benzyl carbamate (**25**), showed similar results to **24** and **26**. In contrast, benzylurea derivative (**27**) exhibited >800-fold selectivity for CDK12 over CDK2. The overlay of the docking model of **27** with CDK12 and the reported crystal structure of CDK2 suggests that this dramatic improvement in selectivity was derived from the steric clash of the benzyl moiety with Lys72 in CDK2 (Figure 9). It is noteworthy that there are apparent differences in selectivity, despite the high similarity of their 2D structures (**27** vs **23** and **25**). We speculated that this difference is dependent on their distinct 3D conformational preferences. The overlay of the single crystal X-ray structures demonstrates that only urea derivative **27** adopts the bent conformation of the benzyl moiety (Figure 10); moreover, this bent conformation is thought to be essential to cause the steric clash with Lys72 of CDK2 (Figure 9). This propensity was confirmed by global conformational preferences in the CSD (Figure 11); that is, only the "C(O)-NH-C-C" substructure (Figure 11 left) tends to adopt a bent conformation, whereas other substructures "C(O)-C-C-C" (Figure 11 middle) and "C(O)-O-C-C" (Figure 11 right) strongly prefer extended conformations. The cyclohexylmethyl analog (**28**) showed similar levels of activity and selectivity to **27**, which implies that it is not the aromaticity or planarity of the benzyl moiety, but the bulkiness that is necessary to weaken CDK2 activity. This is consistent with the assumptions for CDK12 selectivity discussed above (Figure 9). In accordance with the

results for compound **33**, up to 100 μM of the *cis*-isomer (**34**) did not show any CDK12 inhibitory activity.

**Table 3.** SAR of compounds **23**–**28**, and **34**

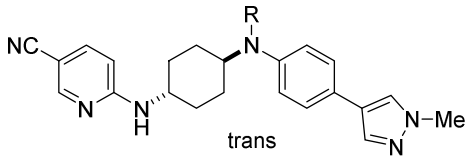


**23–28**

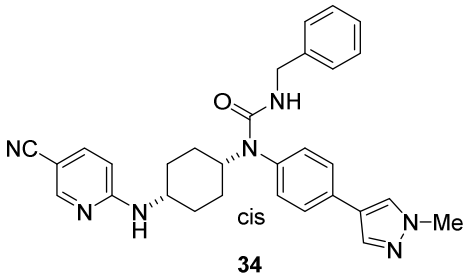


**34**

| Compound | R | CDK12 $IC_{50}$ (μM)[a] | CDK2 $IC_{50}$ (μM)[a] |
|---|---|---|---|
| **24** |  | 0.20 (0.16–0.27) | 1.6 (1.2–2.2) |
| **26** |  | 0.46 (0.36–0.60) | 4.8 (4.1–5.7) |
| **23** | 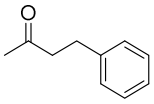 | 0.16 (0.086–0.30) | 2.9 (2.5–3.4) |
| **25** | 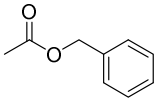 | 0.64 (0.38–1.1) | 2.5 (1.9–3.4) |
| **27** | 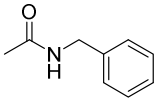 | 0.063 (0.032–0.12) | >100 |
| **28** | 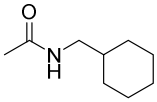 | 0.099 (0.064–0.15) | >100 |
| **34** | | >30 | NT |

[a] $n$ = 2, 95% confidence intervals shown in parentheses. NT = not tested.

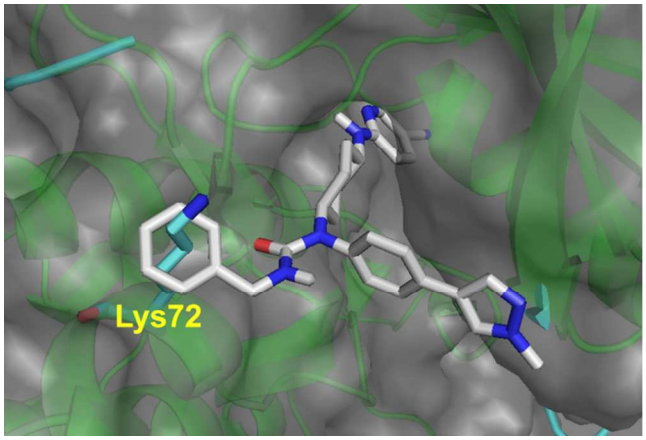


**Figure 9**. Overlay of docking model of **27**/CDK12 (ligand: white, protein: green) and crystal structure of CDK2[43] (2FVD, ligand: omitted, protein: cyan). Lys72 in CDK2 is highlighted.

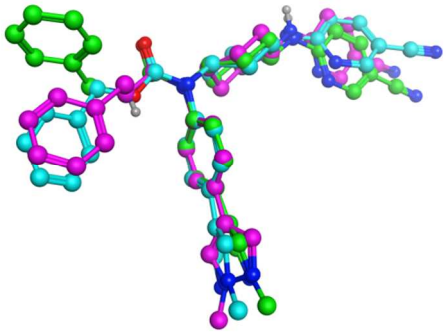

**Figure 10**. Overlay of single crystal X-ray structures of ligands **23** (magenta, CCDC 1835996), **25** (cyan, CCDC 1835997), and **27** (green, CCDC 1835998).

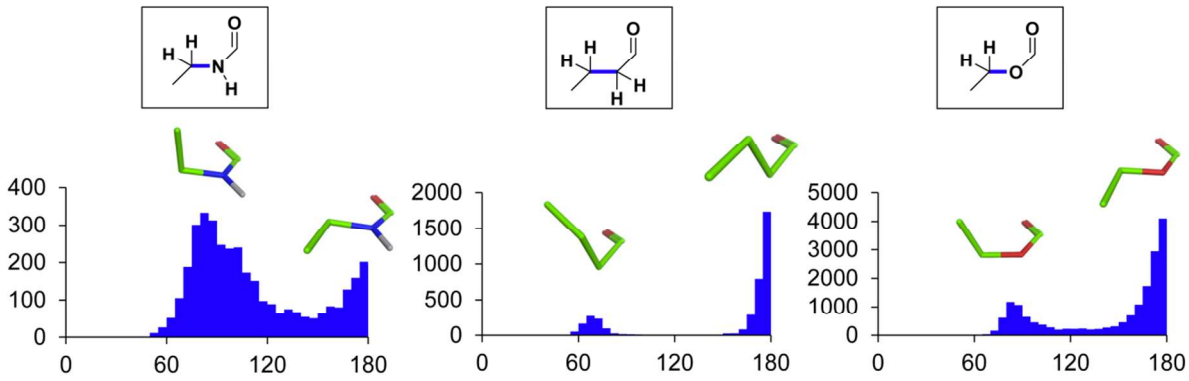


**Figure 11**. Torsion histograms for each substructure in the Cambridge Structural Database. The *x*-axis represents torsion angle bins for the highlighted bonds and the *y*-axis represents occurrence. Substructure queries are depicted above each histogram (cyclic structures around the highlighted bonds were omitted for precise estimation). The histogram for "C(O)-NH-C-C" is illustrated on the left, the histogram for "C(O)-C-C-C" is illustrated in the middle, and the histogram for "C(O)-O-C-C" is illustrated on the right.

Finally, the distal pyrazole ring in **27** was optimized to adjust the physicochemical properties (e.g. solubility) while retaining activity and selectivity. Surprisingly, the truncation of the pyrazole ring (**39**) led to diminished activity (Table 4), although the pyrazole ring of **27** is expected to be solvent-exposed (Figures 8 and 9). The 3-pyridyl derivative (**40**) showed a similar level of potency, selectivity, and solubility as **27**, which also supports the contribution of the distal aromatic ring for activity. These observations imply two possibilities: the pyrazole ring of **27** (or pyridine ring of **40**) might interact with a solvent exposed residue of CDK12 via a water molecule; or, these heterocycles may interact with the C-terminal kinase extension,[9] which is disordered and not defined in the template crystal structure (Supporting information 1). To improve aqueous solubility further, the more hydrophilic methylpyridone ring was employed as a distal ring (**2**, **44**, **46**, and **47**). Among them, compound **2** exhibited the highest aqueous solubility and good permeability with double digit nanomolar CDK12 inhibitory activity and excellent selectivity over CDK2. Although compound **2** is not the best one for selectivity over CDK9, it was considered to be the most suitable molecule for cell-based studies. The selectivity data for known CTD kinases are summarized in Table 4. Compound **2** showed excellent CDK12 selectivity over CDK9, 8, and 7 compared with the non-selective kinase inhibitor staurosporine[44] (Table 5). Meanwhile, **2** turned out to be a strong CDK13 inhibitor, which is reasonable because CDK13 is the closest homolog of CDK12 (92% identity in kinase domain). In contrast, up to 100 μM of compound **34** did not inhibit any of the five CTD kinases tested, including CDK13, thus **34** could be useful as a negative control. The global kinase selectivity of **2** was also investigated (Supporting information 2), and only three out of 441 kinase assays showed ≥80% inhibition at 1 μM compound concentration. As these three kinases (TAOK1, DYRK2, and STK39) are not related to splicing or RNA processing,[45] their inhibition is not likely to disturb the investigation

of RNA biology using **2**. The phosphorylation of CTD Ser2 was evaluated using a ERBB2/HER2 amplified human breast cancer cell line, SK-BR-3. According to the Human Protein Atlas database,[46] CDK12 mRNA is highly expressed in SK-BR-3 cells compared to other cell lines, whereas CDK9 mRNA is expressed at a level similar to other cell lines. Furthermore, the CDK12 gene is co-amplified with the HER2 oncogene in this cell line;[24] therefore, SK-BR-3 is a plausible pathophysiological model for characterization of CDK12 inhibitors as therapeutic agents targeting HER2-positive breast cancer.[25] Table 6 shows that compound **2** inhibited the phosphorylation of the CTD Ser2 in SK-BR-3 cells at low submicromolar concentrations and its degree of inhibition was comparable to the known CDK inhibitor, ibulocydine.[47] In our assay system, ibulocydine showed inhibitory activity for CDK9 and CDK7 consistent with previous reports; however, we noticed that ibulocydine also showed inhibitory activity against CDK12 ($IC_{50}$ values for CDK9, CDK7, and CDK12 were 220, 1200, and 110 nM, respectively). Meanwhile, the negative control **34**[48] (up to 100 μM) did not show any inhibition. In addition to showing inhibitory activity towards Ser2 phosphorylation, compound **2** inhibited the growth of SK-BR-3 cells at submicromolar concentrations.[32] To clarify the mode of inhibition of compound **2**, the time dependency of CDK12 inhibition was investigated by using the known covalent CDK12 inhibitor **3** (THZ-531) as a control (Supporting information 3). Compound **2** did not show any time-dependent inhibition for CDK12, whereas **3** showed clear time dependency as reported.[30] This result suggests compound **2** is a non-covalent CDK12 inhibitor, as expected from its structural features.

**Table 4.** Activity, selectivity, and physicochemical properties of compounds **2**, **27**, **39**, **40**, **44**, **46** and **47**

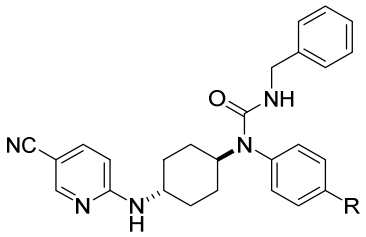

| Compound | R | CDK12 $IC_{50}$ (μM)[a] | CDK2 $IC_{50}$ (μM)[a] | CDK9 $IC_{50}$ (μM)[a] | Solubility at pH 6.8 (μg/mL) | logD at pH 7.4 | PAMPA at pH 7.4 (nm/s) |
|---|---|---|---|---|---|---|---|
| **27** | 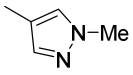 | 0.063 (0.032–0.12) | >100 | >30 | 0.33 | 2.8 | 288 |
| **39** | H | 0.75 (0.36–1.6) | 56 (33–96) | >30 | 4.0 | 3.3 | NT |
| **40** |  | 0.059 (0.014–0.25) | >100 | >30 | 0.67 | 3.0 | 280 |
| **44** | 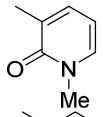 | 0.25 (0.11–0.56) | 18 (10–32) | 15 (11–20) | 4.7 | 2.7 | NT |
| **46** | 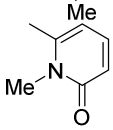 | 0.31 (0.12–0.80) | 27 (15–49) | >30 | <0.090 | 2.6 | NT |
| **47** | 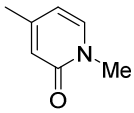 | 0.044 (0.023–0.084) | >100 | >30 | <0.080 | 2.3 | 247 |
| **2** | 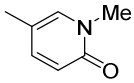 | 0.052 (0.023–0.12) | >100 | 16 (8.4–30) | 7.7 | 2.4 | 273 |

[a] $n = 2$, 95% confidence intervals shown in parentheses. NT = not tested.

**Table 5.** Selectivity over C-terminal domain kinases

| Compound | CDK12 $IC_{50}$ (μM) [a] | CDK9 $IC_{50}$ (μM) [a] | CDK8 $IC_{50}$ (μM) [a] | CDK7 $IC_{50}$ (μM) [a] | CDK13 $IC_{50}$ (μM) [a] |
|---|---|---|---|---|---|
| **2** | 0.052 (0.023–0.12) | 16 (8.4–30) | >10 | >10 | 0.010 (0.0030–0.034) |
| **34** | >30 | >30 | >10 | >10 | >10 |
| **Staurosporine** | 0.053 (0.033–0.086) | 0.014 (0.010–0.021) | 0.015 (0.010–0.022) | 0.12 (0.059–0.23) | 0.057 (0.023–0.14) |

[a] $n = 2$, 95% confidence intervals shown in parentheses.

**Table 6.** Inhibition of C-terminal domain Ser2 phosphorylation and growth inhibition in SK-BR-3 cell

| Compound | CTD Ser2 phosphorylation $IC_{50}$ (nM)[a] | growth inhibition $GI_{50}$ (μM) |
|---|---|---|
| **2** | 195 (± 2.6) | 0.8 (± 0.36) |
| **34** | ND[b] | NT[c] |
| **Ibulocydine** | 259 (± 2.3) | NT[c] |

[a] $n = 4$, SD values shown in parentheses. [b]Not detected up to 100 μM. [c]Not tested.

## Conclusion

We discovered novel and selective CDK12 inhibitors by utilizing experimentally determined conformations in the CSD. The optimized compound **2** showed double digit nanomolar inhibitory activity for CDK12 (and CDK13), good selectivity over other CTD kinases, and excellent physicochemical properties. Furthermore, **2** exhibited high kinome-wide selectivity**,** and inhibited CTD Ser2 phosphorylation in SK-BR-3 cells and cell growth. Compound **2** and the negative control **34** represent valuable chemical probes to study the functions of CDK12 in

splicing, RNA processing, and its other biological roles. In addition, these compounds could serve as a foundation for the development of CDK12 inhibitors as chemotherapeutic agents alone, or in combination with other therapies.

## Experimental section

### Chemistry

**General.** Proton nuclear magnetic resonance ($^1$H NMR) spectra were recorded on Bruker AVANCE-300 (300 MHz), Bruker AVANCE-400 (400 MHz), and Bruker AVANCE-600 (600 MHz), and carbon nuclear magnetic resonance ($^{13}$C NMR) spectra were recorded on Bruker AVANCE-300 (75 MHz) and Bruker AVANCE-600 (151 MHz) in $CDCl_3$ or DMSO-$d_6$ solution. Chemical shifts are given in parts per million (ppm) with tetramethylsilane as an internal standard. Abbreviations are used as follows: s = singlet, d = doublet, t = triplet, m = multiplet, dd = doublet of doublets, tt = triplet of triplets, q = quartet, brs = broad singlet. Coupling constants (*J* values) are given in hertz (Hz). Low-resolution mass spectra (MS) were acquired using an Agilent LC/MS system (Agilent1200SL/Agilent6130MS, Agilent1200SL/Agilent1956MS, or Agilent1200SL/Agilent6110MS) or Shimadzu UFLC/MS (Prominence UFLC high pressure gradient system/LCMS-2020) operating in an electrospray ionization mode (ESI+). The column used was an L-column 2 ODS (3.0 × 50 mm I.D., 3 μm, CERI) with a temperature of 40 °C and a flow rate of 1.2 or 1.5 mL/min. Condition 1: Mobile phases A and B under an acidic condition were 0.05% TFA in water and 0.05% TFA in MeCN, respectively. The ratio of mobile phase B was increased linearly from 5 to 90% over 0.9 min, 90% over the next 1.1 min. Condition 2: Mobile phases A and B under a neutral condition were a mixture of 5 mmol/L $AcONH_4$ and MeCN (9/1, v/v) and a mixture of 5 mmol/L $AcONH_4$ and MeCN (1/9, v/v), respectively. The ratio of mobile phase B was increased linearly from 5 to 90% over 0.9 min, 90% over the next 1.1 min. The purities of all compounds tested in biological systems were assessed as being >95% using elemental analysis or analytical HPLC. Elemental analyses were carried out by Sumika Chemical Analysis Service or Toray Research Center and were within 0.4% of the theoretical

values. Analytical HPLC were carried out using HPLC with NQAD (Nano Quality Analyte Detector) or Corona CAD (Charged Aerosol Detector). The column was an L-column 2 ODS (30 × 2.1 mm I.D., CERI) or a Capcell Pak C18AQ (50 mm × 3.0 mm I.D., Shiseido) with a temperature of 50 °C and a flow rate of 0.5 mL/min. Mobile phases A and B under a neutral condition were a mixture of 50 mmol/L $AcONH_4$, water and MeCN (1/8/1, v/v/v) and a mixture of 50 mmol/L $AcONH_4$ and MeCN (1/9, v/v), respectively. The ratio of mobile phase B was increased linearly from 5 to 95% over 3 min, 95% over the next 1 min. Reaction progress was determined by thin layer chromatography (TLC) analysis on Merck Kieselgel 60 F254 plates or Fuji Silysia NH plates. Chromatographic purification was carried out on silica gel columns ((Merck Kieselgel 60, 70–230 mesh or 230–400 mesh, Merck), (Chromatorex NH-DM 1020, 100–200 mesh, Fuji Silysia Chemical), (Inject column and Universal column, YAMAZEN, http://yamazenusa.com/products/columns/), or (Purif-Pack Si or NH, Shoko Scientific, http://shoko-sc.co.jp/english2/)). Preparative HPLC was performed using a Gilson Preparative HPLC System with UV detector (220 and 254 nm). Mobile phases A and B under a basic condition were 0.0225% aqueous formic acid solution and MeCN, respectively. The ratio of mobile phase B was increased linearly in 15 min. The column used was a Synergi C18 (150 × 25 mm I.D., 10 μm, Phenomenex), and a flow rate of 25 mL/min. All commercially available solvents and reagents were used without further purification. Yields were not optimized. Staurosporine was purchased from Enzo Life Sciences Inc., and Ibulocydine was purchased from Medicilon Inc. (fee for service). **3** (THZ-531) was synthesized according to the literature procedure.[30]

**6-((1-((4-(1-Methyl-*1H*-pyrazol-4-yl)phenyl)sulfonyl)piperidin-4-yl)amino)nicotinonitrile**

**(1).** A mixture of **6** (300 mg, 0.841 mmol), DIPEA (0.879 mL, 5.04 mmol), and 6-fluoronicotinonitrile (308 mg, 2.52 mmol) in NMP (5 mL) was stirred at 120 °C for 7 h. The mixture was poured into water and extracted with EtOAc. The organic layer was separated, washed with water and brine, dried over $MgSO_4$, and concentrated. The residue was purified by NH silica gel column chromatography (hexane/EtOAc = 95/5 to 0/100) and solidified with hexane/EtOH to give **1** (260 mg, 73%) as a white solid. $^1$H NMR (300 MHz, DMSO-$d_6$) δ 1.37–1.60 (m, 2H), 1.86–2.04 (m, 2H), 2.51–2.62 (m, 2H), 3.53 (d, $J$ = 12.1 Hz, 2H), 3.69–3.85 (m, 1H), 3.89 (s, 3H), 6.51 (d, $J$ = 8.9 Hz, 1H), 7.55 (d, $J$ = 7.2 Hz, 1H), 7.59–7.67 (m, 1H), 7.70 (d, $J$ = 8.1 Hz, 2H), 7.82 (d, $J$ = 8.1 Hz, 2H), 8.01 (s, 1H), 8.32 (s, 2H). $^{13}$C NMR (151 MHz, DMSO-$d_6$) δ 30.3 (2C), 38.7, 44.7 (2C), 46.1, 94.5, 118.9, 120.3, 125.2 (2C), 128.1 (2C), 128.9, 132.4, 136.6, 137.3, 138.5, 152.9, 159.1. 1C was not observed. MS $m/z$ 423.2 $(M + H)^+$. *Anal*. Calcd for $C_{21}H_{22}N_6O_2S$: C, 59.70; H, 5.25; N, 19.89. Found: C, 59.58; H, 5.34; N, 19.77.

**3-Benzyl-1-(*trans*-4-((5-cyanopyridin-2-yl)amino)cyclohexyl)-1-(4-(1-methyl-6-oxo-1,6-dihydropyridin-3-yl)phenyl)urea (2).** A mixture of **38** (203 mg, 0.402 mmol), **41** (123 mg, 0.523 mmol), potassium acetate (79 mg, 0.804 mmol), and Pd(dppf)$Cl_2 \cdot CH_2Cl_2$ (32.9 mg, 0.0402 mmol) in NMP (10 mL) was stirred at 100 °C under Ar overnight. The reaction mixture was cooled to room temperature and insoluble materials were filtered off. The filtrate was poured into water and extracted with EtOAc. The organic layer was separated, washed with water and brine, dried over $Na_2SO_4$, and concentrated. The residue was purified by silica gel column chromatography (hexane/EtOAc = 70/30 to 0/100) to give **2** (74 mg, 35%) as a grayish white solid. $^1$H NMR (600 MHz, DMSO-$d_6$) δ 1.07–1.20 (m, 2H), 1.27–1.38 (m, 2H), 1.83 (d, $J$ = 11.4 Hz, 2H), 1.92 (d, $J$ = 11.4 Hz, 2H), 3.45–3.52 (m, 1H), 3.52 (s, 3H), 4.16 (d, $J$ = 5.9 Hz, 2H), 4.30 (tt, $J$ = 12.1, 3.5 Hz, 1H), 5.82 (t, $J$ = 6.1 Hz, 1H), 6.47 (d, $J$ = 8.8 Hz, 1H), 6.50 (d, $J$ = 9.2 Hz, 1H), 7.16–7.20 (m,

3H), 7.22 (d, $J$ = 8.4 Hz, 2H), 7.26–7.29 (m, 2H), 7.47 (d, $J$ = 6.6 Hz, 1H), 7.60 (dd, $J$ = 8.8, 1.8 Hz, 1H), 7.66 (d, $J$ = 8.8 Hz, 2H), 7.87 (dd, $J$ = 9.4, 2.8 Hz, 1H), 8.18 (d, $J$ = 2.9 Hz, 1H), 8.29 (d, $J$ = 1.8 Hz, 1H). $^{13}$C NMR (151 MHz, DMSO-$d_6$) δ 30.1 (2C), 31.2 (2C), 37.0, 43.4, 48.5, 53.1, 93.9, 108.8, 116.9, 119.0, 119.2, 126.0 (2C), 126.2, 126.7 (2C), 127.9 (2C), 131.5 (2C), 135.5, 136.6, 137.5, 138.3, 138.6, 141.1, 153.0, 156.4, 159.1, 161.1. MS $m/z$ 533.3 $(M + H)^+$. *Anal*. Calcd for $C_{32}H_{32}N_6O_2 \cdot 0.5H_2O$: C, 70.96; H, 6.14; N, 15.52. Found: C, 71.02; H, 6.29; N, 15.40.

**1-((4-(1-Methyl-1*H*-pyrazol-4-yl)phenyl)sulfonyl)piperidin-4-amine hydrochloride (6).** To a solution of *tert*-butyl piperidin-4-ylcarbamate (**5**) (2.54 g, 12.7 mmol) and $Et_3N$ (2.65 mL, 19.0 mmol) in THF (100 mL) was added 4-bromobenzenesulfonyl chloride (3.56 g, 14.0 mmol) portionwise at 0 °C. The mixture was stirred at room temperature overnight. The mixture was poured into water and extracted with EtOAc. The organic layer was separated, washed with water and brine, dried over $Na_2SO_4$ and concentrated. The residue was washed with diisopropyl ether and collected by filtration to give *tert*-butyl *N*-(1-(4-bromophenyl)sulfonyl-4-piperidyl)carbamate (5.10 g, 96%) as a white solid. $^1$H NMR (300 MHz, $CDCl_3$) δ 1.42 (s, 9H), 1.48 (dd, $J$ = 12.3, 3.5 Hz, 2H), 1.99 (d, $J$ = 10.5 Hz, 2H), 2.47 (t, $J$ = 12.0 Hz, 2H), 3.40 (brs, 1H), 3.68 (d, $J$ = 11.6 Hz, 2H), 4.38 (brs, 1H), 7.58–7.64 (m, 2H), 7.65–7.72 (m, 2H). MS $m/z$ 441.1 $(M + Na)^+$.

A mixture of *tert*-butyl *N*-(1-(4-bromophenyl)sulfonyl-4-piperidyl)carbamate (5.10 g, 12.2 mmol), 1-methyl-4-(4,4,5,5-tetramethyl-1,3,2-dioxaborolan-2-yl)-1*H*-pyrazole (2.53 g, 12.2 mmol), $Pd(dppf)Cl_2 \cdot CH_2Cl_2$ (993 mg, 1.22 mmol), and $K_2CO_3$ (3.36 g, 24.3 mmol) in DMF (100 mL) and water (20 mL) was stirred at 100 °C under Ar overnight. Insoluble materials were filtered off, and the filtrate was poured into water and extracted with EtOAc. The organic layer was separated, washed with water and brine, dried over $Na_2SO_4$, and concentrated. The residue

was purified by silica gel column chromatography (hexane/EtOAc = 98/2 to 50/50) to give *tert*-butyl (1-((4-(1-methyl-1*H*-pyrazol-4-yl)phenyl)sulfonyl)piperidin-4-yl)carbamate (4.23 g, 83%) as a white solid. $^1$H NMR (300 MHz, DMSO-$d_6$) δ 1.34 (s, 9H), 1.37–1.50 (m, 2H), 1.76 (d, $J$ = 10.4 Hz, 2H), 2.35–2.48 (m, 2H), 3.24 (brs, 1H), 3.47 (d, $J$ = 12.1 Hz, 2H), 3.89 (s, 3H), 6.85 (d, $J$ = 6.1 Hz, 1H), 7.67 (d, $J$ = 8.1 Hz, 2H), 7.80 (d, $J$ = 8.0 Hz, 2H), 8.00 (s, 1H), 8.31 (s, 1H). MS $m/z$ 443.2 $(M + Na)^+$.

A mixture of *tert*-butyl (1-((4-(1-methyl-1*H*-pyrazol-4-yl)phenyl)sulfonyl)piperidin-4-yl)carbamate (3.80 g, 9.04 mmol) and 10% HCl in MeOH (20 mL) was stirred at room temperature for 3 h. The mixture was concentrated. The residue was solidified with diisopropyl ether and collected by filtration to give **6** (3.20 g, 99%) as a white solid. $^1$H NMR (300 MHz, DMSO-$d_6$) δ 1.49–1.69 (m, 2H), 1.92–2.03 (m, 2H), 2.31–2.46 (m, 2H), 2.96–3.14 (m, 1H), 3.65 (d, $J$ = 12.1 Hz, 2H), 3.89 (s, 3H), 7.65–7.73 (m, 2H), 7.77–7.86 (m, 2H), 8.01 (d, $J$ = 0.6 Hz, 1H), 8.07–8.21 (m, 3H), 8.33 (s, 1H). MS $m/z$ 321.1 $(M + H)^+$.

**2-((1-((4-(1-Methyl-1*H*-pyrazol-4-yl)phenyl)sulfonyl)piperidin-4-yl)amino)isonicotinonitrile (7).** Compound **7** was prepared from compound **6** and 2-chloroisonicotinonitrile in a similar manner to that described for compound **1** and obtained in 5% yield as a light brown solid. $^1$H NMR (300 MHz, DMSO-$d_6$) δ 1.38–1.58 (m, 2H), 1.94 (d, $J$ = 10.3 Hz, 2H), 2.52–2.61 (m, 2H), 3.52 (d, $J$ = 12.4 Hz, 2H), 3.60–3.77 (m, 1H), 3.89 (s, 3H), 6.72–6.82 (m, 2H), 7.06 (d, $J$ = 7.3 Hz, 1H), 7.65–7.74 (m, 2H), 7.78–7.88 (m, 2H), 8.01 (s, 1H), 8.10 (d, $J$ = 5.1 Hz, 1H), 8.32 (s, 1H). $^{13}$C NMR (151 MHz, DMSO-$d_6$) δ 30.36 (2C), 38.72, 44.73 (2C), 46.12, 111.54, 117.35, 119.48, 120.30, 125.18 (2C), 128.09 (2C), 128.92, 132.34, 136.63, 137.32, 149.27, 157.79. 1C was not observed. MS $m/z$ 423.2 $(M + H)^+$. *Anal*. Calcd for $C_{21}H_{22}N_6O_2S \cdot 0.25H_2O$: C, 59.07; H,

5.31; N, 19.68. Found: C, 58.84; H, 5.19; N, 19.35.

**6-((1-((4-(1-Methyl-1*H*-pyrazol-4-yl)phenyl)sulfonyl)piperidin-4-yl)amino)pyridine-2-carbonitrile (8).** Compound **8** was prepared from compound **6** and 6-chloro-2-pyridinecarbonitrile in a similar manner to that described for compound **1** and obtained in 6% yield as a light brown solid. $^1$H NMR (300 MHz, DMSO-$d_6$) δ 1.37–1.58 (m, 2H), 1.95 (dd, $J$ = 12.9, 3.5 Hz, 2H), 2.58 (t, $J$ = 10.1 Hz, 2H), 3.51 (d, $J$ = 12.2 Hz, 2H), 3.61–3.76 (m, 1H), 3.89 (s, 3H), 6.72 (dd, $J$ = 8.6, 0.6 Hz, 1H), 7.02 (dd, $J$ = 6.4, 0.6 Hz, 1H), 7.13 (d, $J$ = 7.2 Hz, 1H), 7.49 (dd, $J$ = 8.7, 7.1 Hz, 1H), 7.70 (d, $J$ = 8.4 Hz, 2H), 7.82 (d, $J$ = 8.6 Hz, 2H), 8.01 (d, $J$ = 0.7 Hz, 1H), 8.32 (s, 1H). $^{13}$C NMR (151 MHz, DMSO-$d_6$) δ 30.3 (2C), 38.7, 44.7 (2C), 45.8, 113.8, 117.2, 118.1, 120.3, 125.2 (2C), 128.1 (2C), 128.9, 130.0, 132.4, 136.6, 137.3, 137.3, 158.1. MS $m/z$ 423.2 $(M + H)^+$. *Anal*. Calcd for $C_{21}H_{22}N_6O_2S \cdot 0.5H_2O$: C, 58.45; H, 5.37; N, 19.48. Found: C, 58.68; H, 5.48; N, 19.77.

***N*-(1-((4-(1-Methyl-*1H*-pyrazol-4-yl)phenyl)sulfonyl)piperidin-4-yl)pyridin-2-amine (9).** A mixture of 2-bromopyridine (0.097 mL, 1.02 mmol), **6** (200 mg, 0.560 mmol), $Pd_2(dba)_3$ (27.9 mg, 0.0305 mmol), 2-dicyclohexylphosphino-2'-(*N,N*-dimethylamino)biphenyl (24.0 mg, 0.0610 mmol), and *tert*-BuONa (147 mg, 1.53 mmol) in toluene (4 mL) was stirred at 100 °C overnight. Insoluble materials were filtered off, the filtrate was poured into water and extracted with EtOAc. The organic layer was washed with water and brine, dried over $Na_2SO_4$, and concentrated. The residue was purified by silica gel column chromatography (hexane/EtOAc = 70/30 to 0/100) to give **9** (15 mg, 7%) as a pale yellow solid.

$^1$H NMR (300 MHz, DMSO-$d_6$) δ 1.35–1.55 (m, 2H), 1.87–1.99 (m, 2H), 2.52–2.59 (m, 2H), 3.52 (d, $J$ = 12.1 Hz, 2H), 3.59–3.74 (m, 1H), 3.89 (s, 3H), 6.36–6.46 (m, 3H), 7.25–7.35 (m, 1H), 7.70 (d, $J$ = 8.5 Hz, 2H), 7.82 (d, $J$ = 8.7 Hz, 2H), 7.88 (dd, $J$ = 5.5, 1.3 Hz, 1H), 8.01 (s, 1H), 8.32 (s, 1H). $^{13}$C NMR (151 MHz, DMSO-$d_6$) δ 30.7 (2C), 38.7, 44.8 (2C), 45.9, 108.3,

111.4, 120.3, 125.2 (2C), 128.1 (2C), 128.9, 132.4, 136.4, 136.6, 137.3, 147.3, 157.9. MS *m*/*z* 398.2 $(M + H)^+$. *Anal*. Calcd for $C_{20}H_{23}N_5O_2S \cdot 0.4H_2O$: C, 59.36; H, 5.93; N, 17.31. Found: C, 59.68; H, 6.29; N, 17.08.

**5-Methoxy-*N*-(1-((4-(1-methyl-*1H*-pyrazol-4-yl)phenyl)sulfonyl)piperidin-4-yl)pyridin-2-amine (10).** Compound **10** was prepared from compound **6** and 2-bromo-5-methoxypyridine in a similar manner to that described for compound **9** and obtained in 29% yield as a light gray solid. $^1$H NMR (300 MHz, DMSO-$d_6$) δ 1.29–1.45 (m, 2H), 1.93 (d, $J$ = 10.7 Hz, 2H), 2.41–2.49 (m, 2H), 3.08–3.27 (m, 1H), 3.55 (d, $J$ = 12.0 Hz, 2H), 3.69 (s, 3H), 3.89 (s, 3H), 5.15 (d, $J$ = 8.4 Hz, 1H), 6.54 (d, $J$ = 8.8 Hz, 1H), 7.01 (dd, $J$ = 8.8, 2.9 Hz, 1H), 7.46 (d, $J$ = 2.8 Hz, 1H), 7.70 (d, $J$ = 8.4 Hz, 2H), 7.82 (d, $J$ = 8.4 Hz, 2H), 8.01 (d, $J$ = 0.6 Hz, 1H), 8.32 (s, 1H). $^{13}$C NMR (151 MHz, DMSO-$d_6$) δ 30.8 (2C), 38.7, 44.9 (2C), 48.1, 52.6, 110.1, 120.3, 125.2 (2C), 125.4, 128.1 (2C), 128.9, 129.8, 132.3, 136.6, 137.3, 138.7, 155.5. MS *m*/*z* 428.2 $(M + H)^+$. *Anal*. Calcd for $C_{21}H_{25}N_5O_3S$: C, 59.00; H, 5.89; N, 16.38. Found: C, 58.79; H, 6.17; N, 16.03.

***N*-(1-((4-(1-Methyl-*1H*-pyrazol-4-yl)phenyl)sulfonyl)piperidin-4-yl)-5-(trifluoromethyl)pyridin-2-amine (11).** Compound **11** was prepared from compound **6** and 2-bromo-5-(trifluoromethyl)pyridine in a similar manner to that described for compound **9** and obtained in 29% yield as a pale yellow solid. $^1$H NMR (300 MHz, DMSO-$d_6$) δ 1.41–1.58 (m, 2H), 1.95 (d, $J$ = 10.1 Hz, 2H), 2.52–2.63 (m, 2H), 3.53 (d, $J$ = 12.3 Hz, 2H), 3.70–3.83 (m, 1H), 3.89 (s, 3H), 6.54 (d, $J$ = 9.0 Hz, 1H), 7.28 (d, $J$ = 7.3 Hz, 1H), 7.59 (dd, $J$ = 8.8, 2.4 Hz, 1H), 7.71 (d, $J$ = 8.6 Hz, 2H), 7.82 (d, $J$ = 8.6 Hz, 2H), 8.01 (d, $J$ = 0.7 Hz, 1H), 8.20–8.23 (m, 1H), 8.32 (s, 1H). $^{13}$C NMR (151 MHz, DMSO-$d_6$) δ 30.4 (2C), 38.7, 44.7 (2C), 46.0, 108.2, 112.4 (q, $J_{C–F}$ = 32.1 Hz, 1C), 120.3 , 125.0 (q, $J_{C–F}$ = 270.0 Hz, 1C), 125.2 (2C), 128.1 (2C), 128.9, 132.4, 133.3, 136.6, 137.3, 145.3 (q, $J_{C–F}$ = 4.4 Hz, 1C), 159.80. MS *m*/*z* 466.2 $(M + H)^+$. *Anal*. Calcd

for $C_{21}H_{22}F_3N_5O_2S$: C, 54.18; H, 4.76; N, 15.05. Found: C, 54.20; H, 4.97; N, 14.82.

**4-((1-((4-(1-Methyl-*1H*-pyrazol-4-yl)phenyl)sulfonyl)piperidin-4-yl)amino)benzonitrile (12).** A mixture of 4-fluorobenzonitrile (154 mg, 1.27 mmol), **6** (200 mg, 0.560 mmol), and $K_2CO_3$ (211 mg, 1.53 mmol) in DMSO (4 mL) was stirred at 120 °C for 4 h. The mixture was poured into water and extracted with EtOAc. The organic layer was washed with water and brine, dried over $Na_2SO_4$, and concentrated. The residue was purified by silica gel column chromatography (hexane/EtOAc = 50/50 to 0/100) to give **12** (22 mg, 9%) as a white solid. $^1$H NMR (300 MHz, DMSO-$d_6$) δ 1.32–1.52 (m, 2H), 1.93 (d, $J$ = 10.8 Hz, 2H), 2.52–2.59 (m, 2H), 3.34–3.44 (m, 1H), 3.50–3.63 (m, 2H), 3.89 (s, 3H), 6.53–6.66 (m, 3H), 7.38 (d, $J$ = 8.8 Hz, 2H), 7.70 (d, $J$ = 8.3 Hz, 2H), 7.83 (d, $J$ = 8.7 Hz, 2H), 8.01 (d, $J$ = 0.6 Hz, 1H), 8.32 (brs, 1H). $^{13}$C NMR (75 MHz, DMSO-$d_6$) δ 31.0 (2C), 39.3, 45.4 (2C), 47.7, 96.0, 112.6 (2C), 120.9, 121.0, 125.8 (2C), 128.7 (2C), 129.5, 132.7, 133.8 (2C), 137.2, 137.9, 151.6. MS $m/z$ 422.3 $(M + H)^+$. *Anal*. Calcd for $C_{22}H_{23}N_5O_2S \cdot 0.3H_2O$: C, 61.89; H, 5.57; N, 16.40. Found: C, 62.05; H, 5.77; N, 16.04.

**6-(Methyl(1-((4-(1-methyl-*1H*-pyrazol-4-yl)phenyl)sulfonyl)piperidin-4-yl)amino)nicotinonitrile (13).** To a solution of **1** (50 mg, 0.12 mmol) in THF (1.5 mL) and DMF (0.5 mL) was added 60% NaH (9.5 mg, 0.24 mmol) at 0 °C. After being stirred at 0 °C for 30 min, iodomethane (0.015 mL, 0.24 mmol) was added to the mixture. The mixture was stirred at ambient temperature overnight. The mixture was poured into water and extracted with EtOAc. The organic layer was washed with water and brine, dried over $Na_2SO_4$, and concentrated. The residual solid was suspended in diisopropyl ether and collected by filtration to give **13** (44 mg, 85%) as a yellow solid. $^1$H NMR (300 MHz, DMSO-$d_6$) δ 1.64 (d, $J$ = 10.0 Hz, 2H), 1.73–1.93 (m, 2H), 2.41 (t, $J$ = 11.3 Hz, 2H), 2.88 (s, 3H), 3.77 (d, $J$ = 11.9 Hz, 2H), 3.90 (s, 3H), 4.39 (brs, 1H), 6.78 (d, $J$ = 9.2 Hz, 1H), 7.67–7.87 (m, 5H), 8.02 (s, 1H), 8.33 (s, 1H), 8.40 (d, $J$ = 2.1 Hz,

1H). $^{13}$C NMR (151 MHz, DMSO-$d_6$) δ 27.5 (2C), 29.5, 38.7, 45.6 (2C), 51.4, 94.5, 106.2, 118.8, 120.3, 125.2 (2C), 128.2 (2C), 128.9, 132.1, 136.6, 137.4, 139.5, 152.1, 158.8. MS *m*/*z* 437.3 $(M + H)^+$. *Anal*. Calcd for $C_{22}H_{24}N_6O_2S \cdot 0.4H_2O$: C, 59.55; H, 5.63; N, 18.94. Found: C, 59.93; H, 6.01; N, 19.25.

**6-(Piperidin-4-ylamino)nicotinonitrile dihydrochloride (15).** A mixture of **14** (5.00 g, 25.0 mmol), 6-chloronicotinonitrile (4.15 g, 30.0 mmol), and DIPEA (8.70 mL, 49.9 mmol) in DMF (50 mL) was stirred at 120 °C overnight. The mixture was poured into water at room temperature and extracted with EtOAc. The organic layer was separated, washed with water and brine, dried over $MgSO_4$, and concentrated. The residue was purified by silica gel column chromatography (hexane/EtOAc = 95/5 to 50/50) and solidified with hexane/THF to give tert-butyl 4-((5-cyanopyridin-2-yl)amino)piperidine-1-carboxylate (5.00 g, 66%) as a white solid. $^1$H NMR (300 MHz, $CDCl_3$) δ 1.24–1.53 (m, 11H), 1.90–2.15 (m, 2H), 2.93 (t, *J* = 11.6 Hz, 2H), 3.78–4.23 (m, 3H), 4.85 (d, *J* = 8.2 Hz, 1H), 6.36 (dd, *J* = 8.8, 0.6 Hz, 1H), 7.55 (dd, *J* = 8.8, 2.3 Hz, 1H), 8.34–8.37 (m, 1H). MS *m*/*z* 247.2 $(M + H - 56)^+$.

To a solution of tert-butyl 4-((5-cyanopyridin-2-yl)amino)piperidine-1-carboxylate (1.00 g, 3.31 mmol) in EtOH (15 mL) was added 4 M HCl in EtOAc (19.8 mL, 79.4 mmol) at room temperature. The mixture was stirred at room temperature overnight and concentrated. The residual solid was suspended in EtOAc and collected by filtration to give **15** (0.896 g, 98%) as a white solid. MS *m*/*z* 203.2 $(M + H)^+$.

**6-((1-(4-(1-methyl-1*H*-pyrazol-4-yl)benzoyl)piperidin-4-yl)amino)nicotinonitrile (16).** To a suspension of **15** (450 mg, 1.64 mmol) in THF (10 mL) were added DIPEA (1.42 mL, 8.18 mmol) and 4-bromobenzoyl chloride (431 mg, 1.96 mmol) in THF (5 mL) at 0 °C. The mixture was stirred 0 °C for 2 h. The mixture was poured into water and extracted with EtOAc. The

organic layer was separated, washed with water and brine, dried over $MgSO_4$, and concentrated. The residue was purified by NH silica gel column chromatography (hexane/EtOAc = 90/10 to 20/80) to give 6-((1-(4-bromobenzoyl)piperidin-4-yl)amino)nicotinonitrile (560 mg, 89%) as a white solid. $^1$H NMR (300 MHz, DMSO-$d_6$) δ 1.22–1.58 (m, 2H), 1.80–2.05 (m, 2H), 2.90–3.27 (m, 2H), 3.44–3.68 (m, 1H), 3.96–4.17 (m, 1H), 4.32 (brs, 1H), 6.56 (d, $J$ = 8.8 Hz, 1H), 7.35 (d, $J$ = 8.5 Hz, 2H), 7.52–7.71 (m, 4H), 8.39 (d, $J$ = 2.0 Hz, 1H). MS $m/z$ 385.1, 387.1 $(M + H)^+$.

A mixture of 6-((1-(4-bromobenzoyl)piperidin-4-yl)amino)nicotinonitrile (150 mg, 0.389 mmol), 1-methyl-4-(4,4,5,5-tetramethyl-1,3,2-dioxaborolan-2-yl)-*1H*-pyrazole (97 mg, 0.466 mmol), cesium carbonate (254 mg, 0.780 mmol), and $PdCl_2(Amphos)_2$ (26.2 mg, 0.0390 mmol) in DMF (3 mL) and water (0.3 mL) was heated at 100 °C for 1 h under microwave irradiation. The mixture was poured into water and extracted with EtOAc. The organic layer was separated, washed with water and brine, dried over $MgSO_4$, and concentrated. The residue was purified by silica gel column chromatography (hexane/EtOAc = 80/20 to 0/100) and solidified with hexane/EtOH to give **16** (124 mg, 82%) as a white solid. $^1$H NMR (300 MHz, DMSO-$d_6$) δ 1.24–1.50 (m, 2H), 1.81–2.04 (m, 2H), 2.94–3.24 (m, 2H), 3.57–3.81 (m, 1H), 3.87 (s, 3H), 4.01–4.39 (m, 2H), 6.56 (d, $J$ = 8.9 Hz, 1H), 7.37 (d, $J$ = 7.5 Hz, 2H), 7.58–7.70 (m, 4H), 7.91 (d, $J$ = 0.7 Hz, 1H), 8.19 (s, 1H), 8.38–8.40 (m, 1H). $^{13}$C NMR (151 MHz, DMSO-$d_6$) δ 30.9, 31.7, 38.6, 40.4, 45.9, 47.1, 94.5, 108.7, 118.9, 121.1, 124.6 (2C), 127.4 (2C), 128.1, 133.3, 133.8, 136.2, 138.5, 153.0, 159.1, 168.9. MS $m/z$ 387.3 $(M + H)^+$. *Anal.* Calcd for $C_{22}H_{22}N_6O$: C, 68.38; H, 5.74; N, 21.75. Found: C, 68.41; H, 5.61; N, 21.65.

**6-((1-(4-(1-methyl-1*H*-pyrazol-4-yl)benzyl)piperidin-4-yl)amino)nicotinonitrile (17).** A mixture of **15** (600 mg, 2.18 mmol), 4-bromobenzyl bromide (545 mg, 2.18 mmol), and $K_2CO_3$ (1.51 g, 10.9 mmol) in DMF (15 mL) was stirred at 80 °C overnight. The mixture was poured

into water and extracted with EtOAc. The organic layer was washed with water and brine, dried over $MgSO_4$, and concentrated. The residue was purified by NH silica gel column chromatography (hexane/EtOAc = 90/10 to 0/100) to give 6-((1-(4-bromobenzyl)piperidin-4-yl)amino)nicotinonitrile (780 mg, 96%) as a white solid. $^1$H NMR (300 MHz, $CDCl_3$) δ 1.35–1.62 (m, 2H), 2.02 (dd, *J* = 14.8, 2.5 Hz, 2H), 2.11–2.27 (m, 2H), 2.82 (d, *J* = 12.2 Hz, 2H), 3.47 (s, 2H), 3.72 (brs, 1H), 4.89 (d, *J* = 6.8 Hz, 1H), 6.34 (dd, *J* = 8.8, 0.6 Hz, 1H), 7.20 (d, *J* = 8.4 Hz, 2H), 7.44 (d, *J* = 8.4 Hz, 2H), 7.54 (dd, *J* = 8.8, 2.2 Hz, 1H), 8.34 (dd, *J* = 2.2, 0.6 Hz, 1H). MS *m*/*z* 371.2, 373.2 $(M + H)^+$.

Compound **17** was prepared from compound 6-((1-(4-bromobenzyl)piperidin-4-yl)amino)nicotinonitrile and 1-methyl-4-(4,4,5,5-tetramethyl-1,3,2-dioxaborolan-2-yl)-*1H*-pyrazole in a similar manner to that described for compound **16** and obtained in 61% yield as a white solid. $^1$H NMR (300 MHz, $CDCl_3$) δ 1.47–1.64 (m, 2H), 1.97–2.11 (m, 2H), 2.11–2.29 (m, 2H), 2.75–3.03 (m, 2H), 3.53 (s, 2H), 3.64–3.84 (m, 1H), 3.94 (s, 3H), 4.93 (d, *J* = 7.3 Hz, 1H), 6.34 (dd, *J* = 8.8, 0.5 Hz, 1H), 7.30 (d, *J* = 8.4 Hz, 2H), 7.38–7.46 (m, 2H), 7.54 (dd, *J* = 8.8, 2.2 Hz, 1H), 7.60 (s, 1H), 7.75 (d, *J* = 0.6 Hz, 1H), 8.34 (d, *J* = 1.8 Hz, 1H). $^{13}$C NMR (151 MHz, DMSO-$d_6$) δ 31.4 (2C), 38.6, 47.4, 51.8 (2C), 61.8, 94.1, 108.8, 119.0, 121.7, 124.7 (2C), 127.5, 129.2 (2C), 131.2, 135.8, 136.1, 138.3, 153.1, 159.2. MS *m*/*z* 373.3 $(M + H)^+$. *Anal*. Calcd for $C_{22}H_{24}N_6 \cdot 0.75H_2O$: C, 68.46; H, 6.66; N, 21.77. Found: C, 68.81; H, 6.65; N, 21.44.

***tert*-Butyl (*trans*-4-((4-bromophenyl)amino)cyclohexyl)carbamate (19).** A mixture of **18** (1.50 g, 7.00 mmol), 1-bromo-4-iodobenzene (1.98 g, 7.00 mmol), *tert*-BuONa (1.01 g, 10.5 mmol), Xantphos (0.486 g, 0.840 mmol) in toluene (30 mL) was degassed and purged with Ar. To the mixture was added $Pd_2(dba)_3$ (0.385 g, 0.420 mmol) at room temperature, and the mixture was

stirred at 80 °C under Ar overnight. The mixture was poured into water and extracted with EtOAc. The organic layer was separated, washed with water and brine, dried over $MgSO_4$, and concentrated. The residue was purified by silica gel column chromatography (hexane/EtOAc = 95/5 to 40/60) and NH silica gel column chromatography (hexane/EtOAc = 95/5 to 30/70) to give **19** (1.16 g, 45%) as a white solid. $^1$H NMR (300 MHz, $CDCl_3$) δ 1.06–1.34 (m, 4H), 1.45 (s, 9H), 1.94–2.23 (m, 4H), 3.04–3.24 (m, 1H), 3.33–3.64 (m, 2H), 4.32–4.47 (m, 1H), 6.44 (d, *J* = 8.7 Hz, 2H), 7.22 (d, *J* = 8.7 Hz, 2H). MS *m*/*z* 369.1, 371.1 $(M + H)^+$.

***tert*-Butyl (*trans*-4-((4-(1-methyl-*1H*-pyrazol-4-yl)phenyl)amino)cyclohexyl)carbamate (20).** A mixture of **19** (1.67 g, 4.52 mmol), 1-methyl-4-(4,4,5,5-tetramethyl-1,3,2-dioxaborolan-2-yl)-1*H*-pyrazole (1.41 g, 6.78 mmol), cesium carbonate (2.95 g, 9.04 mmol) in DMF (30 mL) and water (3 mL) was degassed and purged with Ar. To the mixture was added $PdCl_2(Amphos)_2$ (0.304 g, 0.451 mmol) at room temperature, and the mixture was stirred at 100 °C under Ar overnight. The mixture was poured into water at room temperature and extracted with EtOAc. The organic layer was separated, washed with water and brine, dried over $MgSO_4$ and concentrated. The residue was purified by silica gel column chromatography (hexane/EtOAc = 95/5 to 20/80) to give **20** (1.41 g, 84%) as a white solid. $^1$H NMR (300 MHz, $CDCl_3$) δ 1.10–1.30 (m, 4H), 1.45 (s, 9H), 2.00–2.25 (m, 4H), 3.06–3.31 (m, 1H), 3.36–3.61 (m, 2H), 3.91 (s, 3H), 4.29–4.53 (m, 1H), 6.58 (d, *J* = 8.3 Hz, 2H), 7.21–7.32 (m, 2H), 7.47 (s, 1H), 7.65 (s, 1H). MS *m*/*z* 371.2 $(M + H)^+$.

***N*-(*trans*-4-((5-Cyanopyridin-2-yl)amino)cyclohexyl)-*N*-(4-(1-methyl-1*H*-pyrazol-4-yl)phenyl)acetamide (21).** To a solution of **20** (550 mg, 1.48 mmol) in THF (20 mL) were added DIPEA (1.29 mL, 7.42 mmol) and acetyl chloride (0.317 mL, 4.45 mmol) at 0 °C. The mixture was stirred at 0 °C for 3 h. The mixture was poured into water and extracted with EtOAc. The organic layer

was separated, washed with water and brine, dried over $MgSO_4$, and concentrated. The residue was solidified with hexane/EtOAc to give *tert*-butyl (*trans*-4-(*N*-(4-(1-methyl-1*H*-pyrazol-4-yl)phenyl)acetamido)cyclohexyl)carbamate (482 mg, 79%) as a white solid. $^1$H NMR (300 MHz, $CDCl_3$) δ 1.09–1.34 (m, 4H), 1.40 (s, 9H), 1.77 (s, 3H), 1.85 (d, $J$ = 9.9 Hz, 2H), 1.94–2.06 (m, 2H), 3.07–3.29 (m, 1H), 3.97 (s, 3H), 4.24–4.40 (m, 1H), 4.51–4.67 (m, 1H), 7.04 (d, $J$ = 8.2 Hz, 2H), 7.48 (d, $J$ = 8.2 Hz, 2H), 7.64 (s, 1H), 7.78 (s, 1H). MS $m/z$ 413.2 $(M + H)^+$.

A mixture of *tert*-butyl (*trans*-4-(*N*-(4-(1-methyl-1*H*-pyrazol-4-yl)phenyl)acetamido)cyclohexyl)carbamate (150 mg, 0.364 mmol) and TFA (2.24 mL, 29.1 mmol) was stirred at room temperature for 30 min. The mixture was concentrated and azeotroped with toluene. The residue was neutralized with saturated aqueous $NaHCO_3$, extracted with EtOAc/2-propanol (4/1). The organic layer was separated, washed with water and brine, dried over $MgSO_4$, and concentrated. A mixture of the residue, 6-chloronicotinonitrile (55.6 mg, 0.401 mmol), and DIPEA (0.318 mL, 1.82 mmol) in DMF (5 mL) was stirred at 120 °C overnight. The mixture was poured into water and extracted with EtOAc. The organic layer was separated, washed with water and brine, dried over $MgSO_4$, and concentrated. The residue was purified by silica gel column chromatography (hexane/EtOAc = 20/80 to 0/100) and solidified with hexane/EtOAc to give **21** (29 mg, 19% for 2 steps) as a white solid. $^1$H NMR (600 MHz, DMSO-$d_6$) δ 1.10–1.21 (m, 2H), 1.29–1.38 (m, 2H), 1.66 (s, 3H), 1.81 (d, $J$ = 11.4 Hz, 2H), 1.93 (d, $J$ = 11.0 Hz, 2H), 3.51 (brs, 1H), 3.88 (s, 3H), 4.44 (tt, $J$ = 12.0, 3.4 Hz, 1H), 6.48 (d, $J$ = 9.2 Hz, 1H), 7.18 (d, $J$ = 8.4 Hz, 2H), 7.46 (d, $J$ = 6.2 Hz, 1H), 7.58–7.66 (m, 3H), 7.90 (s, 1H), 8.18 (s, 1H), 8.29 (d, $J$ = 2.2 Hz, 1H). $^{13}$C NMR (151 MHz, DMSO-$d_6$) δ 23.1, 29.4 (2C), 31.1 (2C), 38.6, 48.4, 52.3, 94.0, 119.0, 121.0, 125.5 (2C), 128.0,

130.4 (2C), 132.5, 136.2, 136.9, 153.0, 159.2, 168.6. 2C were not observed. MS *m*/*z* 415.2 $(M + H)^+$. *Anal*. Calcd for $C_{24}H_{26}N_6O \cdot 0.5\ C_4H_8O_2 \cdot H_2O$: C, 65.53; H, 6.77; N, 17.63. Found: C, 65.59; H, 6.46; N, 17.55. Purity 97.8% (HPLC).

***N*-(*trans*-4-((5-Cyanopyridin-2-yl)amino)cyclohexyl)-*N*-(4-(1-methyl-1*H*-pyrazol-4-yl)phenyl)methanesulfonamide (22).** To a solution of **20** (550 mg, 1.48 mmol) in pyridine (15 mL) was added methanesulfonyl chloride (1.15 mL, 14.9 mmol) at room temperature. The mixture was stirred at room temperature overnight. The mixture was concentrated, poured into water and extracted with EtOAc. The organic layer was separated, washed with water and brine, dried over $MgSO_4$, and concentrated. The residue was solidified with hexane/EtOAc to give *tert*-butyl (*trans*-4-((4-(1-methyl-1*H*-pyrazol-4-yl)phenyl)(methylsulfonyl)amino)cyclohexyl)carbamate (541 mg, 81%) as a pale yellow solid. $^1$H NMR (300 MHz, $CDCl_3$) δ 1.10–1.38 (m, 4H), 1.40 (s, 9H), 1.92–2.11 (m, 4H), 2.96 (s, 3H), 3.06–3.31 (m, 1H), 3.97 (s, 3H), 4.03–4.22 (m, 1H), 4.26–4.39 (m, 1H), 7.22 (d, *J* = 8.3 Hz, 2H), 7.48 (d, *J* = 8.3 Hz, 2H), 7.62 (s, 1H), 7.76 (s, 1H). MS *m*/*z* 449.2 $(M + H)^+$.

Compound **22** was prepared from *tert*-butyl (*trans*-4-((4-(1-methyl-1*H*-pyrazol-4-yl)phenyl)(methylsulfonyl)amino)cyclohexyl)carbamate and 6-chloronicotinonitrile in a similar manner to that described for compound **21** and obtained in 23% yield for 2 steps as a pale yellow solid. $^1$H NMR (600 MHz, DMSO-$d_6$) δ 1.20–1.29 (m, 2H), 1.32–1.43 (m, 2H), 1.89–2.01 (m, 4H), 3.09 (s, 3H), 3.48 (brs, 1H), 3.88 (s, 3H), 3.96 (tt, *J* = 11.9, 3.7 Hz, 1H), 6.48 (d, *J* = 8.8 Hz, 1H), 7.24 (d, *J* = 8.4 Hz, 2H), 7.47 (d, *J* = 7.0 Hz, 1H), 7.56–7.65 (m, 3H), 7.89 (d, *J* = 0.7 Hz, 1H), 8.18 (s, 1H), 8.28 (d, *J* = 2.2 Hz, 1H). $^{13}$C NMR (151 MHz, DMSO-$d_6$) δ 30.8 (2C), 31.0 (2C), 38.6, 40.5, 48.2, 57.0, 94.0, 119.0, 121.0, 125.3 (2C), 128.1, 132.4 (2C), 132.9, 133.1, 136.2, 138.4, 153.0, 159.2. 1C was not observed. MS *m*/*z*

451.2 $(M + H)^+$. *Anal*. Calcd for $C_{23}H_{26}N_6O_2S$: C, 61.31; H, 5.82; N, 18.65. Found: C, 61.20; H, 5.74; N, 18.28.

**_N_-(*trans*-4-((5-cyanopyridin-2-yl)amino)cyclohexyl)-_N_-(4-(1-methyl-*1H*-pyrazol-4-yl)phenyl)-3-phenylpropanamide (23).** *tert*-Butyl (*trans*-4-((4-(1-methyl-1*H*-pyrazol-4-yl)phenyl)(3-phenylpropanoyl)amino)cyclohexyl)carbamate was prepared from compound **20** and 3-phenylpropionyl chloride in a similar manner to that described for compound **21** and obtained in 86% yield as a white solid. $^1$H NMR (300 MHz, DMSO-$d_6$) δ 0.91–1.11 (m, 2H), 1.25 (d, $J$ = 12.7 Hz, 2H), 1.34 (s, 9H), 1.66–1.83 (m, 4H), 2.12 (t, $J$ = 7.6 Hz, 2H), 2.73 (t, $J$ = 7.6 Hz, 2H), 2.94 (brs, 1H), 3.86 (s, 3H), 4.37 (t, $J$ = 11.6 Hz, 1H), 6.67 (d, $J$ = 8.0 Hz, 1H), 7.01 (t, $J$ = 7.7 Hz, 4H), 7.08–7.25 (m, 3H), 7.56 (d, $J$ = 8.1 Hz, 2H), 7.87 (s, 1H), 8.15 (s, 1H). MS $m/z$ 525.3 $(M + Na)^+$.

A mixture of *tert*-butyl (*trans*-4-((4-(1-methyl-1*H*-pyrazol-4-yl)phenyl)(3-phenylpropanoyl)amino)cyclohexyl)carbamate (170 mg, 0.338 mmol) and 4 M HCl in EtOAc (2.0 mL, 8.00 mmol) was stirred at room temperature. After being stirred at room temperature for 2 h, the mixture was concentrated. A mixture of the residue, 6-fluoronicotinonitrile (124 mg, 1.01 mmol), and DIPEA (0.295 mL, 1.69 mmol) in NMP (2 mL) was stirred at 80 °C overnight. The mixture was poured into water and extracted with EtOAc. The organic layer was separated, washed with water and brine, dried over $Na_2SO_4$, and concentrated. The residue was purified by silica gel column chromatography (hexane/EtOAc = 80/20 to 20/80) to give **23** (130 mg, 76%) as a white solid. $^1$H NMR (600 MHz, DMSO-$d_6$) δ 1.08–1.17 (m, 2H), 1.28–1.40 (m, 2H), 1.78 (d, $J$ = 11.4 Hz, 2H), 1.93 (d, $J$ = 11.4 Hz, 2H), 2.15 (t, $J$ = 7.7 Hz, 2H), 2.75 (t, $J$ = 7.5 Hz, 2H), 3.50 (brs, 1H), 3.87 (s, 3H), 4.47 (tt, $J$ = 12.1, 3.5 Hz, 1H), 6.48 (d, $J$ = 9.2 Hz, 1H), 6.99–7.07 (m, 4H), 7.10–7.16 (m, 1H), 7.18–7.23

(m, 2H), 7.46 (d, *J* = 5.9 Hz, 1H), 7.57 (d, *J* = 8.4 Hz, 2H), 7.60 (dd, *J* = 9.0, 1.7 Hz, 1H), 7.88 (s, 1H), 8.16 (s, 1H), 8.28 (d, *J* = 2.2 Hz, 1H). $^{13}$C NMR (151 MHz, DMSO-$d_6$) δ 29.4 (2C), 30.9, 31.1 (2C), 36.3, 38.6, 48.4, 52.5, 94.0, 108.8, 119.0, 120.9, 125.5 (2C), 125.8, 128.0, 128.1 (2C), 128.1 (2C), 130.5 (2C), 132.5, 136.1, 136.2, 138.3, 141.1, 153.0, 159.2, 170.3. MS *m*/*z* 505.3 $(M + H)^+$. *Anal*. Calcd for $C_{31}H_{32}N_6O \cdot 0.5C_6H_{14}O \cdot 0.5H_2O$: C, 72.31; H, 7.14; N, 14.88. Found: C, 72.53; H, 7.29; N, 15.20. Purity 98.8% (HPLC).

**Methyl (*trans*-4-((5-cyanopyridin-2-yl)amino)cyclohexyl)(4-(1-methyl-*1H*-pyrazol-4-yl)phenyl)carbamate (24).** To a solution of **20** (300 mg, 0.809 mmol) and DIPEA (0.423 mL, 2.43 mmol) in $CH_2Cl_2$ (5 mL) was added methyl chloroformate (0.336 mL, 4.34 mmol) at room temperature. The mixture was stirred for 16 h at room temperature. To the mixture was added water, and the mixture was extracted with $CH_2Cl_2$. The organic layers was separated, dried over $Na_2SO_4$, and concentrated. The residue was purified by silica gel column chromatography (petroleum ether/EtOAc = 3/1 to 2/1) to give methyl (*trans*-4-((*tert*-butoxycarbonyl)amino)cyclohexyl)(4-(1-methyl-*1H*-pyrazol-4-yl)phenyl)carbamate (350 mg, 85%) as a white solid. MS *m*/*z* 429.2 $(M + H)^+$.

Compound **24** was prepared from methyl (*trans*-4-((*tert*-butoxycarbonyl)amino)cyclohexyl)(4-(1-methyl-*1H*-pyrazol-4-yl)phenyl)carbamate and 6-fluoronicotinonitrile in a similar manner to that described for compound **23** and obtained in 33% yield for 2 steps as a white solid. $^1$H NMR (400 MHz, DMSO-$d_6$) δ 1.16–1.39 (m, 4H), 1.81–1.99 (m, 4H), 3.51–3.52 (m, 4H), 3.87 (s, 3H), 4.02–4.13 (m, 1H), 6.48 (d, *J* = 8.8 Hz, 1H), 7.11 (d, *J* = 8.4 Hz, 2H), 7.49 (d, *J* = 6.4 Hz, 1H), 7.55 (d, *J* = 8.4 Hz, 2H), 7.61 (d, *J* = 8.8 Hz, 1H), 7.87 (s, 1H), 8.15 (s, 1H), 8.30 (d, *J* = 2.0 Hz, 1H). $^{13}$C NMR (151 MHz, DMSO-$d_6$) δ 29.7

(2C), 31.0 (2C), 38.6, 48.4, 52.3, 55.5, 94.0, 108.8, 119.0, 121.2, 125.2 (2C), 127.9, 130.2 (2C), 131.8, 135.9, 136.1, 138.3, 153.0, 155.1, 159.2. MS *m*/*z* 431.2 $(M + H)^+$. *Anal*. Calcd for $C_{24}H_{26}N_6O_2 \cdot H_2O$: C, 64.27; H, 6.29; N, 18.74. Found: C, 64.49; H, 6.37; N, 18.82.

**Benzyl (*trans*-4-((5-cyanopyridin-2-yl)amino)cyclohexyl)(4-(1-methyl-*1H*-pyrazol-4-yl)phenyl)carbamate (25).** Benzyl (*trans*-4-((*tert*-butoxycarbonyl)amino)cyclohexyl)(4-(1-methyl-*1H*-pyrazol-4-yl)phenyl)carbamate was prepared from compound **20** and benzyl chloroformate in a similar manner to that described for compound **24** and obtained in 62% yield as a white solid. MS *m*/*z* 449.2 $(M + H)^+$. Compound **25** was prepared from benzyl (*trans*-4-((*tert*-butoxycarbonyl)amino)cyclohexyl)(4-(1-methyl-*1H*-pyrazol-4-yl)phenyl)carbamate and 6-fluoronicotinonitrile in a similar manner to that described for compound **23** and obtained in 37% yield for 2 steps as a white solid. $^1$H NMR (600 MHz, DMSO-$d_6$) δ 1.20–1.43 (m, 4H), 1.81–2.03 (m, 4H), 3.54 (brs, 1H), 3.87 (s, 3H), 4.06–4.14 (m, 1H), 5.05 (s, 2H), 6.48 (d, *J* = 8.8 Hz, 1H), 7.14 (d, *J* = 8.4 Hz, 2H), 7.17–7.24 (m, 2H), 7.23–7.29 (m, 1H), 7.29–7.34 (m, 2H), 7.46 (d, *J* = 5.5 Hz, 1H), 7.57 (d, *J* = 8.4 Hz, 2H), 7.61 (dd, *J* = 8.8, 1.5 Hz, 1H), 7.87 (brs, 1H), 8.14 (s, 1H), 8.30 (d, *J* = 2.2 Hz, 1H).$^{13}$C NMR (151 MHz, DMSO-$d_6$) δ 29.7 (2C), 31.0 (2C), 38.6, 48.4, 55.7, 65.9, 94.0, 108.9, 119.0, 121.2, 125.1 (2C), 126.8 (2C), 127.5, 127.9, 128.2 (2C), 130.1 (2C), 131.9, 135.8, 136.1, 137.0, 138.4, 153.0, 154.4, 159.2. MS *m*/*z* 507.2 $(M + H)^+$. *Anal*. Calcd for $C_{30}H_{30}N_6O_2 \cdot 0.5H_2O$: C, 69.88; H, 6.06; N, 16.30. Found: C, 69.54; H, 6.12; N, 16.44.

**1-(*trans*-4-((5-Cyanopyridin-2-yl)amino)cyclohexyl)-3-ethyl-1-(4-(1-methyl-*1H*-pyrazol-4-yl)phenyl)urea (26).** To a solution of **20** (300 mg, 0.809 mmol) in THF (10 mL) was added ethyl isocyanate (0.077 mL, 0.972 mmol) at room temperature. The mixture was stirred at room

temperature for 60 h. The precipitate solid was collected by filtration to give *tert*-butyl (*trans*-4-((ethylcarbamoyl)(4-(1-methyl-1*H*-pyrazol-4-yl)phenyl)amino)cyclohexyl)carbamate (210 mg, 53%) as a white solid. $^1$H NMR (400 MHz, $CDCl_3$) δ 1.00 (t, *J* = 7.2 Hz, 3H), 1.17–1.29 (m, 4H), 1.41 (s, 9H),1.88 (d, *J* = 12.0 Hz, 2H), 1.98 (d, *J* = 12.0 Hz, 2H), 3.14–3.20 (m, 3H), 3.91 (t, *J* = 5.6 Hz, 1H), 3.98 (s, 3H), 4.34–4.36 (m, 1H), 4.45–4.52 (m, 1H), 7.10 (d, *J* = 8.4 Hz, 2H), 7.50 (d, *J* = 8.4 Hz, 2H), 7.65 (s, 1H), 7.79 (d, *J* = 0.4 Hz, 1H). MS *m*/*z* 442.3 $(M + H)^+$.

A mixture of *tert*-butyl (*trans*-4-((ethylcarbamoyl)(4-(1-methyl-1*H*-pyrazol-4-yl)phenyl)amino)cyclohexyl)carbamate (220 mg, 0.498 mmol) and 4 M HCl in dioxane (10 mL, 40.0 mmol) was stirred at room temperature for 2 h, and then the mixture was concentrated. To a solution of the residue and 6-bromonicotinonitrile (167 mg, 0.913 mmol) in DMF (10 mL) was added cesium carbonate (595 mg, 1.83 mmol) at room temperature. The mixture was stirred at 100 °C for 6 h. Insoluble materials were filtered off, and the filtrate was concentrated. The residue was purified by preparative HPLC (0.0225% aqueous formic acid solution/MeCN = 54/46 to 24/76) to give **26** (39 mg, 15% for 2 steps) as a brown solid. $^1$H NMR (600 MHz, DMSO-$d_6$) δ 0.91 (t, *J* = 7.0 Hz, 3H), 1.07–1.17 (m, 2H), 1.27–1.38 (m, 2H), 1.79 (d, *J* = 11.4 Hz, 2H), 1.91 (d, *J* = 11.0 Hz, 2H), 2.94–3.03 (m, 2H), 3.49 (brs, 1H), 3.88 (s, 3H), 4.23-4.32 (m, 1H), 5.12 (t, *J* = 5.7 Hz, 1H), 6.47 (d, *J* = 8.8 Hz, 1H), 7.10 (d, *J* = 8.1 Hz, 2H), 7.46 (d, *J* = 5.5 Hz, 1H), 7.58–7.64 (m, 3H), 7.89 (s, 1H), 8.16 (s, 1H), 8.28 (d, *J* = 2.2 Hz, 1H). $^{13}$C NMR (151 MHz, DMSO-$d_6$) δ 15.6, 30.1 (2C), 31.3 (2C), 34.8, 38.6, 48.5, 52.9, 93.9, 108.9, 119.0, 121.3, 125.7 (2C), 127.9, 131.4 (2C), 132.1, 135.8, 136.1, 138.3, 153.0, 156.3, 159.2. MS *m*/*z* 444.2 $(M + H)^+$. *Anal*. Calcd for $C_{25}H_{29}N_7O \cdot 0.5H_2O$: C, 66.35; H, 6.68; N, 21.67. Found: C, 66.19; H, 6.64; N, 21.90.

**3-Benzyl-1-(*trans*-4-((5-cyanopyridin-2-yl)amino)cyclohexyl)-1-(4-(1-methyl-*1H*-pyrazol-4-yl)phenyl)urea (27).** To a solution of **20** (500 mg, 1.35 mmol) and $Et_3N$ (0.563 mL, 4.05 mmol) in THF (12 mL) was added benzyl isocyanate (0.500 mL, 4.05 mmol) at room temperature. The mixture was stirred at room temperature overnight. The mixture was poured into water at room temperature. The resultant precipitated solid was collected by filtration. The resultant colorless solid was dissolved in THF and purified by NH silica gel column chromatography (hexane/EtOAc = 90/10 to 0/100) and solidified with hexane/EtOAc to give *tert*-butyl (*trans*-4-((benzylcarbamoyl)(4-(1-methyl-1*H*-pyrazol-4-yl)phenyl)amino)cyclohexyl)carbamate (610 mg, 90%) as a white solid. $^1$H NMR (300 MHz, DMSO-$d_6$) δ 0.94–1.16 (m, 2H), 1.17–1.31 (m, 2H), 1.34 (s, 9H), 1.75 (d, $J$ = 10.1 Hz, 4H), 2.83–3.02 (m, 1H), 3.87 (s, 3H), 4.07–4.27 (m, 3H), 5.77 (t, $J$ = 5.6 Hz, 1H), 6.66 (d, $J$ = 7.3 Hz, 1H), 7.09–7.20 (m, 5H), 7.22–7.31 (m, 2H), 7.62 (d, $J$ = 8.1 Hz, 2H), 7.88 (s, 1H), 8.16 (s, 1H). MS $m/z$ 504.3 $(M + H)^+$.

Compound **27** was prepared from *tert*-butyl (*trans*-4-((benzylcarbamoyl)(4-(1-methyl-1*H*-pyrazol-4-yl)phenyl)amino)cyclohexyl)carbamate and 6-fluoronicotinonitrile in a similar manner to that described for compound **23** and obtained in 82% yield as a white solid. $^1$H NMR (300 MHz, DMSO-$d_6$) δ 1.02–1.23 (m, 2H), 1.25–1.43 (m, 2H), 1.81 (d, $J$ = 10.1 Hz, 2H), 1.92 (d, $J$ = 11.3 Hz, 2H), 3.50 (brs, 1H), 3.87 (s, 3H), 4.15 (d, $J$ = 6.0 Hz, 2H), 4.29 (t, $J$ = 11.5 Hz, 1H), 5.81 (t, $J$ = 5.9 Hz, 1H), 6.47 (d, $J$ = 9.1 Hz, 1H), 7.09–7.21 (m, 5H), 7.24–7.34 (m, 2H), 7.46 (d, $J$ = 7.2 Hz, 1H), 7.57–7.66 (m, 3H), 7.89 (s, 1H), 8.17 (s, 1H), 8.28 (d, $J$ = 1.6 Hz, 1H). $^{13}$C NMR (151 MHz, DMSO-$d_6$) δ 30.1 (2C), 31.3 (2C), 38.6, 43.4, 48.5, 53.1, 93.9, 109.0, 119.0, 121.2, 125.7 (2C), 126.1, 126.6 (2C), 127.86, 127.91 (2C), 131.4 (2C), 132.2, 135.6, 136.1, 138.3, 141.2, 153.0, 156.4, 159.2. MS $m/z$ 506.3 $(M + H)^+$. *Anal.* Calcd for $C_{30}H_{31}N_7O$: C, 71.26; H, 6.18; N, 19.39. Found: C, 71.07; H, 6.24; N, 19.40.

**1-(*trans*-4-((5-Cyanopyridin-2-yl)amino)cyclohexyl)-3-(cyclohexylmethyl)-1-(4-(1-methyl-*1H*-pyrazol-4-yl)phenyl)urea (28).** *tert*-Butyl (*trans*-4-(((cyclohexylmethyl)carbamoyl)(4-(1-methyl-1*H*-pyrazol-4-yl)phenyl)amino)cyclohexyl)carbamate was prepared from compound **20** and cyclohexanemethyl isocyanate in a similar manner to that described for compound **27** and obtained in 69% yield as a white solid. $^1$H NMR (300 MHz, DMSO-$d_6$) δ 0.60–0.84 (m, 2H), 0.90–1.31 (m, 8H), 1.34 (s, 9H), 1.44–1.66 (m, 5H), 1.66–1.83 (m, 4H), 2.79 (t, $J$ = 6.1 Hz, 2H), 2.86–3.03 (m, 1H), 3.87 (s, 3H), 4.16 (t, $J$ = 11.8 Hz, 1H), 4.96 (t, $J$ = 5.6 Hz, 1H), 6.65 (d, $J$ = 7.4 Hz, 1H), 7.07 (d, $J$ = 8.0 Hz, 2H), 7.61 (d, $J$ = 8.1 Hz, 2H), 7.89 (s, 1H), 8.17 (s, 1H). MS $m/z$ 510.4 $(M + H)^+$.

Compound **28** was prepared from *tert*-butyl (*trans*-4-(((cyclohexylmethyl)carbamoyl)(4-(1-methyl-1*H*-pyrazol-4-yl)phenyl)amino)cyclohexyl)carbamate and 6-fluoronicotinonitrile in a similar manner to that described for compound **23** and obtained in 48% yield as a white solid. $^1$H NMR (300 MHz, DMSO-$d_6$) δ 0.61–0.82 (m, 2H), 0.95–1.20 (m, 5H), 1.23–1.41 (m, 3H), 1.44–1.67 (m, 5H), 1.79 (d, $J$ = 10.9 Hz, 2H), 1.91 (d, $J$ = 10.3 Hz, 2H), 2.80 (t, $J$ = 6.1 Hz, 2H), 3.49 (brs, 1H), 3.88 (s, 3H), 4.26 (t, $J$ = 11.8 Hz, 1H), 5.00 (t, $J$ = 5.7 Hz, 1H), 6.47 (d, $J$ = 8.9 Hz, 1H), 7.10 (d, $J$ = 8.2 Hz, 2H), 7.46 (d, $J$ = 7.8 Hz, 1H), 7.55–7.67 (m, 3H), 7.90 (s, 1H), 8.18 (s, 1H), 8.28 (d, $J$ = 1.9 Hz, 1H). $^{13}$C NMR (75 MHz, DMSO-$d_6$) δ 25.9 (2C), 26.7, 30.7 (2C), 30.8 (2C), 31.8 (2C), 38.3, 46.7, 49.1, 53.5, 94.5, 119.6, 121.8, 126.2 (2C), 128.5, 131.9 (2C), 132.7, 136.3, 136.7, 138.9, 153.6, 156.9, 159.7. 2C were not observed. MS $m/z$ 512.4 $(M + H)^+$. *Anal*. Calcd for $C_{30}H_{37}N_7O$: C, 70.42; H, 7.29; N, 19.16. Found: C, 70.42; H, 7.30; N, 19.23.

***N*-(4-(1-Methyl-*1H*-pyrazol-4-yl)phenyl)-*N*-(*trans*-4-(quinazolin-2-ylamino)cyclohexyl)acetamide (29).** A mixture of *tert*-butyl

(*trans*-4-(*N*-(4-(1-methyl-1*H*-pyrazol-4-yl)phenyl)acetamido)cyclohexyl)carbamate (105 mg, 0.255 mmol) and TFA (1.57 mL, 20.4 mmol) was stirred at room temperature for 15 min. The mixture was concentrated and azeotroped with toluene. The residue was basified with saturated aqueous $NaHCO_3$ at room temperature and extracted with EtOAc/2-propanol (4:1). The organic layer was separated, washed with water and brine, dried over $MgSO_4$ and concentrated. A mixture of the residue, 2-chloroquinazoline (62.8 mg, 0.381 mmol), and DBU (0.114 mL, 0.762 mmol) in DMF (3 mL) was stirred at 120 °C for 4 h. The mixture was poured into water at room temperature and extracted with EtOAc. The organic layer was separated, washed with water and brine, dried over $MgSO_4$ and concentrated. The residue was purified by NH silica gel column chromatography (hexane/EtOAc = 95/5 to 0/100) and solidified with hexane/EtOH to give **29** (41 mg, 37%) as a white solid. $^1$H NMR (300 MHz, DMSO-$d_6$) δ 1.05–1.27 (m, 2H), 1.31–1.54 (m, 2H), 1.67 (s, 3H), 1.83 (d, $J$ = 11.6 Hz, 2H), 1.99 (d, $J$ = 11.6 Hz, 2H), 3.52–3.72 (m, 1H), 3.89 (s, 3H), 4.46 (t, $J$ = 11.6 Hz, 1H), 7.10–7.29 (m, 4H), 7.38 (d, $J$ = 8.4 Hz, 1H), 7.54–7.70 (m, 3H), 7.74 (d, $J$ = 7.8 Hz, 1H), 7.93 (s, 1H), 8.21 (s, 1H), 9.05 (s, 1H). $^{13}$C NMR (75 MHz, DMSO-$d_6$) δ 23.7, 30.2 (2C), 31.7 (2C), 49.0, 53.0, 112.0, 121.6, 122.2, 125.2, 126.1 (2C), 128.3, 128.6, 131.1 (2C), 133.0, 134.4, 136.8, 137.5, 152.1, 159.3, 162.5, 169.1. 1C was not observed. MS *m*/*z* 441.2 $(M + H)^+$. *Anal*. Calcd for $C_{26}H_{28}N_6O \cdot 0.1H_2O$: C, 70.60; H, 6.43; N, 19.00. Found: C, 70.51; H, 6.23; N, 18.93.

**6-((*trans*-4-((4-(1-Methyl-1*H*-pyrazol-4-yl)phenyl)amino)cyclohexyl)amino)nicotinonitrile (30).** Compound **30** was prepared from compound **20** and 6-fluoronicotinonitrile in a similar manner to that described for compound **23** and obtained in 42% yield as a colorless solid. $^1$H NMR (300 MHz, DMSO-$d_6$) δ 1.12–1.47 (m, 4H), 2.00 (t, J = 11.7 Hz, 4H), 3.21 (d, $J$ = 7.4 Hz, 1H), 3.70–3.90 (m, 4H), 5.37 (d, $J$ = 8.2 Hz, 1H), 6.47–6.63 (m, 3H), 7.24 (d, $J$ = 8.3 Hz, 2H),

7.53 (d, $J$ = 7.2 Hz, 1H), 7.59–7.71 (m, 2H), 7.85 (s, 1H), 8.38 (d, $J$ = 1.8 Hz, 1H). $^{13}$C NMR (75 MHz, DMSO-$d_6$) δ 31.4 (2C), 31.7 (2C), 39.0, 49.5, 50.8, 94.5, 113.2 (2C), 119.7, 120.4, 123.2, 126.4 (2C), 126.5, 135.5, 138.9, 146.9, 153.7, 159.8. 1C was not observed. MS $m/z$ 373.2 $(M + H)^+$. *Anal*. Calcd for $C_{22}H_{24}N_6$: C, 70.94; H, 6.49; N, 22.56. Found: C, 70.74; H, 6.32; N, 22.71.

***tert*-Butyl (*cis*-4-((4-(1-methyl-*1H*-pyrazol-4-yl)phenyl)amino)cyclohexyl)carbamate (32).** *tert*-Butyl (*cis*-4-((4-bromophenyl)amino)cyclohexyl)carbamate was prepared from **31** and 1-bromo-4-iodobenzene in a similar manner to that described for compound **19** and obtained in 26% yield as a white solid. $^1$H NMR (300 MHz, $CDCl_3$) δ 1.45 (s, 9H), 1.57–1.66 (m, 4H), 1.69–1.88 (m, 4H), 3.40 (brs, 1H), 3.54–3.76 (m, 2H), 4.54 (brs, 1H), 6.46 (d, $J$ = 8.7 Hz, 2H), 7.23 (d, $J$ = 8.7 Hz, 2H). MS $m/z$ 369.1, 371.1 $(M + H)^+$.

Compound **32** was prepared from *tert*-butyl (*cis*-4-((4-bromophenyl)amino)cyclohexyl)carbamate and 1-methyl-4-(4,4,5,5-tetramethyl-1,3,2-dioxaborolan-2-yl)-*1H*-pyrazole in a similar manner to that described for compound **20** and obtained in 96% yield as a white solid. $^1$H NMR (300 MHz, $CDCl_3$) δ 1.45 (s, 9H), 1.59–1.68 (m, 4H), 1.70–1.89 (m, 4H), 3.47 (brs, 1H), 3.55–3.74 (m, 2H), 3.91 (s, 3H), 4.45–4.69 (m, 1H), 6.59 (d, $J$ = 8.3 Hz, 2H), 7.22–7.30 (m, 2H), 7.47 (s, 1H), 7.65 (s, 1H). MS $m/z$ 371.2 $(M + H)^+$.

***N*-(*cis*-4-((5-Cyanopyridin-2-yl)amino)cyclohexyl)-*N*-(4-(1-methyl-1*H*-pyrazol-4-yl)phenyl)acetamide (33).** *tert*-Butyl (*cis*-4-(acetyl(4-(1-methyl-1*H*-pyrazol-4-yl)phenyl)amino)cyclohexyl)carbamate was prepared from compound **32** and acetyl chloride in a similar manner to that described for compound **21** and obtained in 89% yield as a white solid. $^1$H NMR (300 MHz, $CDCl_3$) δ 1.13–1.32 (m, 2H), 1.39 (s, 9H), 1.63–1.87 (m, 9H), 3.78 (brs, 1H), 3.98 (s, 3H), 4.40–4.69 (m, 2H), 7.08 (d, $J$ = 7.8

Hz, 2H), 7.52 (d, *J* = 8.1 Hz, 2H), 7.66 (s, 1H), 7.79 (s, 1H). MS *m*/*z* 313.2 $(M - Boc + H)^+$.

Compound **33** was prepared from *tert*-butyl *(cis*-4-(acetyl(4-(1-methyl-1*H*-pyrazol-4-yl)phenyl)amino)cyclohexyl)carbamate and 6-fluoronicotinonitrile in a similar manner to that described for compound **23** and obtained in 82% yield as a white solid. $^1$H NMR (300 MHz, DMSO-$d_6$) δ 1.25–1.45 (m, 2H), 1.54–1.73 (m, 7H), 1.89 (d, *J* = 13.4 Hz, 2H), 3.88 (s, 3H), 3.94 (brs, 1H), 4.45 (t, *J* = 11.5 Hz, 1H), 6.54 (d, *J* = 8.9 Hz, 1H), 7.19 (d, *J* = 7.9 Hz, 2H), 7.34 (d, *J* = 5.5 Hz, 1H), 7.56 (dd, *J* = 9.0, 1.2 Hz, 1H), 7.63 (d, *J* = 8.0 Hz, 2H), 7.91 (s, 1H), 8.19 (s, 1H), 8.33 (d, *J* = 1.7 Hz, 1H). $^{13}$C NMR (151 MHz, DMSO-$d_6$) δ 23.1, 25.8 (2C), 28.8 (2C), 38.6, 44.4, 53.1, 94.1, 108.9, 119.0, 121.0, 125.6 (2C), 128.0, 130.5 (2C), 132.4, 136.1, 137.2, 138.0, 152.8, 159.3, 168.5. MS *m*/*z* 415.2 $(M + H)^+$. *Anal*. Calcd for $C_{24}H_{26}N_6O$: C, 69.54; H, 6.32; N, 20.27. Found: C, 69.36; H, 6.42; N, 19.98.

**3-Benzyl-1-(*cis*-4-((5-cyanopyridin-2-yl)amino)cyclohexyl)-1-(4-(1-methyl-1*H*-pyrazol-4-yl) phenyl)urea (34).** *tert*-Butyl (*cis*-4-((benzylcarbamoyl)(4-(1-methyl-1*H*-pyrazol-4-yl)phenyl)amino)cyclohexyl)carbamate was prepared from compound **32** and benzyl isocyanate in a similar manner to that described for compound **27** and obtained in 68% yield as a white solid. $^1$H NMR (300 MHz, DMSO-$d_6$) δ 1.32 (s, 9H), 1.34–1.58 (m, 6H), 1.71 (d, *J* = 13.5 Hz, 2H), 3.46 (brs, 1H), 3.87 (s, 3H), 4.10–4.27 (m, 3H), 5.67 (t, *J* = 6.0 Hz, 1H), 6.63 (brs, 1H), 7.10–7.20 (m, 5H), 7.22–7.31 (m, 2H), 7.62 (d, *J* = 8.3 Hz, 2H), 7.89 (s, 1H), 8.16 (s, 1H). MS *m*/*z* 526.2 $(M + Na)^+$.

Compound **34** was prepared from *tert*-butyl (*cis*-4-((benzylcarbamoyl)(4-(1-methyl-1*H*-pyrazol-4-yl)phenyl)amino)cyclohexyl)carbamate and 6-fluoronicotinonitrile in a similar manner to that described for compound **23** and obtained in 52% yield as a white solid. $^1$H NMR (300 MHz, DMSO-$d_6$) δ 1.27–1.46 (m, 2H), 1.52–1.72 (m,

4H), 1.89 (d, $J$ = 12.1 Hz, 2H), 3.87 (s, 3H), 3.93 (brs, 1H), 4.15 (d, $J$ = 6.1 Hz, 2H), 4.27 (t, $J$ = 11.7 Hz, 1H), 5.71 (t, $J$ = 5.9 Hz, 1H), 6.54 (d, $J$ = 8.9 Hz, 1H), 7.11–7.21 (m, 5H), 7.22–7.37 (m, 3H), 7.56 (dd, $J$ = 8.8, 2.2 Hz, 1H), 7.63 (d, $J$ = 8.3 Hz, 2H), 7.89 (s, 1H), 8.17 (s, 1H), 8.33 (d, $J$ = 2.2 Hz, 1H). $^{13}$C NMR (151 MHz, DMSO-$d_6$) δ 26.5 (2C), 29.0 (2C), 38.6, 43.4, 44.4, 54.0, 94.0, 108.8, 119.0, 121.3, 125.8 (2C), 126.1, 126.6 (2C), 127.8, 127.9 (2C), 131.4 (2C), 132.1, 135.9, 136.1, 138.0, 141.2, 152.8, 156.4, 159.3. MS $m/z$ 506.2 $(M + H)^+$. *Anal*. Calcd for $C_{30}H_{31}N_7O \cdot 0.5C_4H_8O_2$: C, 69.92; H, 6.42; N, 17.84. Found: C, 69.59; H, 6.70; N, 17.80. Purity 98.1% (HPLC).

***tert*-Butyl (*trans*-4-((benzylcarbamoyl)(4-bromophenyl)amino)cyclohexyl)carbamate (35).** Compound **35** was prepared from compound **19** and benzyl isocyanate in a similar manner to that described for compound **27** and obtained in 93% yield as a white solid. $^1$H NMR (300 MHz, DMSO-$d_6$) δ 0.88–1.12 (m, 2H), 1.14–1.31 (m, 2H), 1.34 (s, 9H), 1.67–1.82 (m, 4H), 2.85–3.04 (m, 1H), 4.07–4.24 (m, 3H), 5.98 (t, $J$ = 5.8 Hz, 1H), 6.66 (d, $J$ = 7.5 Hz, 1H), 7.07–7.20 (m, 5H), 7.23–7.31 (m, 2H), 7.62 (d, $J$ = 8.3 Hz, 2H). MS $m/z$ 502.2, 504.2 $(M + H)^+$.

***tert*-Butyl (*trans*-4-((benzylcarbamoyl)(phenyl)amino)cyclohexyl)carbamate (36).** A mixture of **35** (157 mg, 0.312 mmol), $Et_3N$ (0.065 mL, 0.468 mmol), and 10% Pd/C (33.3 mg, 0.0312 mmol) in EtOH (3 mL) and THF (3 mL) was purged with $H_2$. The mixture was stirred at room temperature under $H_2$ for 3 h. The catalyst was removed by filtration, and the filtrate was concentrated. The residue was purified by NH silica gel column chromatography (hexane/EtOAc = 95/5 to 20/80) and solidified with hexane/EtOAc to give **36** (133 mg, quantitative) as a white solid. $^1$H NMR (300 MHz, DMSO-$d_6$) δ 0.85–1.28 (m, 4H), 1.34 (s, 9H), 1.74 (d, $J$ = 10.5 Hz, 4H), 2.90 (brs, 1H), 4.10–4.24 (m, 3H), 5.65 (t, $J$ = 6.0 Hz, 1H), 6.67 (d, $J$ = 8.2 Hz, 1H), 7.04–7.32 (m, 7H), 7.36–7.52 (m, 3H). MS $m/z$ 424.2 $(M + H)^+$.

***tert*-Butyl (*trans*-4-((benzylcarbamoyl)(4-(pyridin-3-yl)phenyl)amino)cyclohexyl)carbamate (37).** Compound **37** was prepared from compound **35** and 3-pyridinylboronic acid in a similar manner to that described for compound **20** and obtained in 95% yield as a white solid. $^1$H NMR (300 MHz, DMSO-$d_6$) δ 0.96–1.37 (m, 4H), 1.34 (s, 9H), 1.66–1.90 (m, 4H), 2.95 (d, $J$ = 6.5 Hz, 1H), 4.09–4.35 (m, 3H), 5.91 (t, $J$ = 6.0 Hz, 1H), 6.58–6.76 (m, 1H), 7.09–7.21 (m, 3H), 7.22–7.37 (m, 4H), 7.50 (dd, $J$ = 7.9, 4.8 Hz, 1H), 7.83 (d, $J$ = 8.2 Hz, 2H), 8.13 (d, $J$ = 8.0 Hz, 1H), 8.59 (d, $J$ = 4.7 Hz, 1H), 8.94 (d, $J$ = 1.8 Hz, 1H). MS $m/z$ 501.3 $(M + H)^+$.

**3-Benzyl-1-(4-bromophenyl)-1-(*trans*-4-((5-cyanopyridin-2-yl)amino)cyclohexyl)urea (38).** Compound **38** was prepared from compound **35** and 6-fluoronicotinonitrile in a similar manner to that described for compound **23** and obtained in 80% yield as a white solid. $^1$H NMR (300 MHz, DMSO-$d_6$) δ 0.93–1.19 (m, 2H), 1.24–1.42 (m, 2H), 1.79 (d, $J$ = 11.6 Hz, 2H), 1.91 (d, $J$ = 10.5 Hz, 2H), 3.49 (brs, 1H), 4.14 (d, $J$ = 5.8 Hz, 2H), 4.27 (t, $J$ = 12.0 Hz, 1H), 6.02 (t, $J$ = 5.9 Hz, 1H), 6.47 (d, $J$ = 8.9 Hz, 1H), 7.11–7.21 (m, 5H), 7.23–7.31 (m, 2H), 7.46 (d, $J$ = 7.2 Hz, 1H), 7.57–7.67 (m, 3H), 8.30 (d, $J$ = 2.0 Hz, 1H). MS $m/z$ 504.2, 506.1 $(M + H)^+$.

**3-Benzyl-1-(*trans*-4-((5-cyanopyridin-2-yl)amino)cyclohexyl)-1-phenylurea (39).** Compound **39** was prepared from compound **36** and 6-fluoronicotinonitrile in a similar manner to that described for compound **23** and obtained in 71% yield as a white solid. $^1$H NMR (300 MHz, DMSO-$d_6$) δ 1.01–1.19 (m, 2H), 1.23–1.42 (m, 2H), 1.81 (d, $J$ = 11.3 Hz, 2H), 1.91 (d, $J$ = 10.8 Hz, 2H), 3.48 (brs, 1H), 4.16 (d, $J$ = 5.9 Hz, 2H), 4.28 (t, $J$ = 12.0 Hz, 1H), 5.69 (t, $J$ = 6.0 Hz, 1H), 6.47 (d, $J$ = 8.9 Hz, 1H), 7.18 (t, $J$ = 8.2 Hz, 5H), 7.23–7.32 (m, 2H), 7.37–7.52 (m, 4H), 7.60 (dd, $J$ = 8.8, 2.0 Hz, 1H), 8.29 (d, $J$ = 2.1 Hz, 1H). $^{13}$C NMR (151 MHz, DMSO-$d_6$) δ 30.1 (2C), 31.2 (2C), 43.4, 48.5, 53.1, 93.9, 108.8, 119.0, 126.2, 126.6 (2C), 127.9, 127.9 (2C), 129.3 (2C), 131.0 (2C), 138.0, 138.4, 141.1, 153.0, 156.3, 159.2. MS $m/z$ 426.2 $(M + H)^+$. *Anal*. Calcd

for $C_{26}H_{27}N_5O$: C, 73.39; H, 6.40; N, 16.46. Found: C, 73.73; H, 6.44; N, 16.61.

**3-Benzyl-1-(*trans*-4-((5-cyanopyridin-2-yl)amino)cyclohexyl)-1-(4-(pyridin-3-yl)phenyl)urea (40).** Compound **40** was prepared from compound **37** and 6-fluoronicotinonitrile in a similar manner to that described for compound **23** and obtained in 53% yield as a white solid. $^1$H NMR (300 MHz, DMSO-$d_6$) δ 1.08–1.25 (m, 2H), 1.26–1.42 (m, 2H), 1.79–1.98 (m, 4H), 3.43–3.58 (m, 1H), 4.17 (d, $J$ = 5.9 Hz, 2H), 4.26–4.38 (m, 1H), 5.94 (t, $J$ = 6.1 Hz, 1H), 6.47 (d, $J$ = 8.9 Hz, 1H), 7.14–7.23 (m, 3H), 7.27 (d, $J$ = 6.9 Hz, 2H), 7.32 (d, $J$ = 8.1 Hz, 2H), 7.44–7.54 (m, 2H), 7.60 (dd, $J$ = 8.8, 1.9 Hz, 1H), 7.84 (d, $J$ = 8.2 Hz, 2H), 8.13 (d, $J$ = 8.2 Hz, 1H), 8.29 (d, $J$ = 2.0 Hz, 1H), 8.59 (d, $J$ = 4.7 Hz, 1H), 8.95 (d, $J$ = 1.8 Hz, 1H). $^{13}$C NMR (151 MHz, DMSO-$d_6$) δ 30.2 (2C), 31.3 (2C), 43.5, 48.5, 53.3, 93.9, 108.9, 119.0, 123.8, 126.2, 126.7 (2C), 127.7, 127.9 (2C), 131.8 (2C), 134.0 (2C), 134.7, 136.4, 138.1, 138.3, 141.2, 147.6, 148.6, 153.0, 156.3, 159.2. MS $m/z$ 503.3 $(M + H)^+$. *Anal*. Calcd for $C_{31}H_{30}N_6O \cdot 0.2\ C_4H_8O_2$: C, 73.42; H, 6.12; N, 16.15. Found: C, 73.25; H, 5.97; N, 16.07. Purity 99.7% (HPLC).

**3-Benzyl-1-(*trans*-4-((5-cyanopyridin-2-yl)amino)cyclohexyl)-1-(4-(1-methyl-2-oxo-1,2-dihydropyridin-3-yl)phenyl)urea (44).** Compound **44** was prepared from compound **38** and 1-methyl-3-(4,4,5,5-tetramethyl-1,3,2-dioxaborolan-2-yl)pyridin-2(1*H*)-one (**42**) in a similar manner to that described for compound **2** and obtained in 69% yield as a white solid. $^1$H NMR (600 MHz, DMSO-$d_6$) δ 1.10–1.21 (m, 2H), 1.28–1.38 (m, 2H), 1.83 (d, $J$ = 11.4 Hz, 2H), 1.92 (d, $J$ = 11.7 Hz, 2H), 3.43–3.60 (m, 4H), 4.18 (d, $J$ = 5.9 Hz, 2H), 4.30 (tt, $J$ = 12.0, 3.6 Hz, 1H), 5.79 (t, $J$ = 5.9 Hz, 1H), 6.34 (t, $J$ = 6.8 Hz, 1H), 6.47 (d, $J$ = 8.8 Hz, 1H), 7.15–7.22 (m, 5H), 7.24–7.30 (m, 2H), 7.46 (d, $J$ = 6.2 Hz, 1H), 7.60 (dd, $J$ = 9.0, 2.0 Hz, 1H), 7.69 (dd, $J$ = 7.0, 2.2 Hz, 1H), 7.76 (dd, $J$ = 6.8, 2.0 Hz, 1H), 7.82 (d, $J$ = 8.8 Hz, 2H), 8.29 (d, $J$ = 1.8 Hz, 1H). $^{13}$C NMR (151 MHz, DMSO-$d_6$) δ 30.2 (2C), 31.2 (2C), 37.4, 43.4, 48.5, 53.3, 93.9, 105.1, 108.8,

119.0, 126.2, 126.6 (2C), 127.9 (2C), 128.1, 129.0 (2C), 130.4 (2C), 136.3, 137.0, 137.9, 138.3, 139.4, 141.1, 153.0, 156.4, 159.2, 160.7. MS *m*/*z* 533.2 $(M + H)^+$. *Anal*. Calcd for $C_{32}H_{32}N_6O_2 \cdot C_4H_8O_2$: C, 69.66; H, 6.50; N, 13.54. Found: C, 69.54; H, 6.81; N, 13.80. Purity 99.6% (HPLC).

**3-Benzyl-1-(*trans*-4-((5-cyanopyridin-2-yl)amino)cyclohexyl)-1-(4-(4,4,5,5-tetramethyl-1,3,2-dioxaborolan-2-yl)phenyl)urea (45).** A mixture of **38** (2.40 g, 4.76 mmol), potassium acetate (1.87 g, 19.0 mmol), **43** (2.42 g, 9.52 mmol), and $Pd(dppf)Cl_2$ (0.696 g, 0.95 mmol) in DMSO (40 mL) was degassed and purged with $N_2$ three times. The mixture was stirred at 80 °C under $N_2$ for 2.5 h. The mixture was poured into water at room temperature and extracted with EtOAc. The organic layer was separated, washed with water and brine, dried over $MgSO_4$, and concentrated. The residue was purified by silica gel column chromatography (hexane/EtOAc = 90/10 to 20/80), and the resultant product was washed with hexane and collected by filtration to give **45** (2.31 g, 88%) as a white solid. $^1$H NMR (300 MHz, DMSO-$d_6$) δ 1.08–1.43 (m, 16H), 1.71–1.85 (m, 2H), 1.86–1.98 (m, 2H), 3.41–3.55 (m, 1H), 4.13 (d, *J* = 5.9 Hz, 2H), 4.29 (t, *J* = 11.7 Hz, 1H), 5.81 (t, *J* = 6.2 Hz, 1H), 6.46 (d, *J* = 8.9 Hz, 1H), 7.10–7.22 (m, 5H), 7.23–7.32 (m, 2H), 7.46 (d, *J* = 7.6 Hz, 1H), 7.60 (dd, *J* = 8.9, 2.4 Hz, 1H), 7.76 (d, *J* = 8.2 Hz, 2H), 8.28 (d, *J* = 1.9 Hz, 1H). MS *m*/*z* 552.3 $(M + H)^+$.

**3-Benzyl-1-(*trans*-4-((5-cyanopyridin-2-yl)amino)cyclohexyl)-1-(4-(1-methyl-6-oxo-1,6-dihydropyridin-2-yl)phenyl)urea (46).** Compound **46** was prepared from compound **45** and 6-bromo-1-methylpyridin-2(*1H*)-one in a similar manner to that described for compound **20** and obtained in 44% yield as a white solid. $^1$H NMR (600 MHz, DMSO-$d_6$) δ 1.13–1.23 (m, 2H), 1.30–1.40 (m, 2H), 1.85 (d, *J* = 11.4 Hz, 2H), 1.94 (d, *J* = 11.0 Hz, 2H), 3.32 (s, 3H), 3.48–3.61 (m, 1H), 4.20 (d, *J* = 5.9 Hz, 2H), 4.32 (tt, *J* = 12.1, 3.5 Hz, 1H), 5.98 (t, *J* = 6.1 Hz, 1H), 6.19

(dd, *J* = 6.8, 1.3 Hz, 1H), 6.45 (dd, *J* = 9.0, 1.3 Hz, 1H), 6.48 (d, *J* = 8.8 Hz, 1H), 7.16–7.22 (m, 3H), 7.27–7.32 (m, 4H), 7.43–7.51 (m, 2H), 7.56 (d, *J* = 8.1 Hz, 2H), 7.61 (d, *J* = 7.7 Hz, 1H), 8.30 (d, *J* = 2.2 Hz, 1H). $^{13}$C NMR (151 MHz, DMSO-$d_6$) δ 30.1 (2C), 31.3 (2C), 34.1, 43.4, 48.4, 53.4, 94.0, 107.0, 108.9, 117.9, 119.0, 126.2, 126.5 (2C), 128.0 (2C), 129.5 (2C), 131.2 (2C), 134.5, 138.3, 138.8, 138.9, 141.1, 149.6, 153.0, 156.3, 159.1, 162.3. MS *m*/*z* 533.2 $(M + H)^+$. *Anal*. Calcd for $C_{32}H_{32}N_6O_2 \cdot 0.5H_2O$: C, 70.96; H, 6.14; N, 15.52. Found: C, 71.10; H, 6.01; N, 15.52.

**3-Benzyl-1-(*trans*-4-((5-cyanopyridin-2-yl)amino)cyclohexyl)-1-(4-(1-methyl-2-oxo-1,2-dihydropyridin-4-yl)phenyl)urea (47).** Compound **47** was prepared from compound **45** and 4-bromo-1-methylpyridin-2(1*H*)-one in a similar manner to that described for compound **20** and obtained in 48% yield as a white solid. $^1$H NMR (600 MHz, $CDCl_3$) δ 1.28–1.36 (m, 2H), 1.39–1.48 (m, 2H), 2.00 (d, *J* = 11.7 Hz, 2H), 2.12 (d, *J* = 11.7 Hz, 2H), 3.56 (brs, 1H), 3.60 (s, 3H), 4.28–4.35 (m, 1H), 4.38 (d, *J* = 5.5 Hz, 2H), 4.62 (tt, *J* = 12.1, 3.5 Hz, 1H), 5.10 (d, *J* = 7.7 Hz, 1H), 6.28 (d, *J* = 8.8 Hz, 1H), 6.40 (dd, *J* = 7.0, 1.8 Hz, 1H), 6.79 (d, *J* = 1.8 Hz, 1H), 7.18 (d, *J* = 7.3 Hz, 2H), 7.20–7.24 (m, 1H), 7.25–7.30 (m, 4H), 7.38 (d, *J* = 7.3 Hz, 1H), 7.42 (dd, *J* = 9.0, 2.0 Hz, 1H), 7.62 (d, *J* = 8.4 Hz, 2H), 8.27 (d, *J* = 1.8 Hz, 1H). $^{13}$C NMR (151 MHz, $CDCl_3$) δ 30.5 (2C), 32.2 (2C), 37.4, 44.7, 49.4, 53.7, 96.5, 105.1, 107.6, 117.4, 118.7, 127.1 (2C), 127.2, 128.2 (2C), 128.6 (2C), 131.8 (2C), 138.0, 138.5, 138.9, 139.2, 139.5, 150.4, 153.2, 156.7, 159.0, 163.1. MS *m*/*z* 533.2 $(M + H)^+$. *Anal*. Calcd for $C_{32}H_{32}N_6O_2 \cdot 0.4H_2O$: C, 71.20; H, 6.12; N, 15.57. Found: C, 71.36; H, 6.10; N, 15.40.

**Evaluation of solubility.** Small volumes of compound solution dissolved in DMSO were added to the aqueous buffer solution (pH 6.8). After incubation, precipitates were separated by filtration. The solubility was determined by UV absorbance of each filtrate.

**Parallel artificial membrane permeability assay (PAMPA).** The donor wells were filled with 200 μL of PRISMA HT buffer (pH 7.4, pION inc.) containing 10 μmol/L test compound. The filter on the bottom of each acceptor well was coated with 4 μL of a GIT-0 Lipid Solution (pION Inc.) and filled with 200 μL of Acceptor Sink Buffer (pION inc.). The acceptor filter plate was put on the donor plate and incubated for 3 h at room temperature. After the incubation, the amount of test compound in both the donor and acceptor wells was measured by LC/MS/MS.

**Evaluation of LogD.** LogD7.4, which is a partition coefficient between 1-octanol and aqueous buffer pH 7.4, of the compounds was measured on the chromatographic procedure whose condition was developed based on a published method.[49,50]

**Biology**

**Reagents.** Human GST-tagged CDK2/CCNA2 (04-103), GST-tagged CDK7/CycH/MAT1 (04-108), GST-tagged CDK8/CycC (04-109), and GST-tagged CDK9/CycT1 (04-110) were obtained from Carna Biosciences (Kobe, Japan). LANCE detection buffer, ULight-4E-BP1(Thr37/Thr46) substrate peptide, and Eu-labeled anti-phospho-eIF4E-binding protein 1 (Thr37/46) antibody were purchased from PerkinElmer (Waltham, MA).

**Preparation of human full-length CDK12.** Human full-length CDK12 was prepared in-house by a baculovirus expression system. Human CDK12 (residues 1–1490 aa, full, Genbank Accession No. NM_016507) was co-expressed with human CycK (residues 1–580 aa, full,

Genbank Accession No. NM_001099402) in Sf9 cells by using a baculovirus expression system. CDK12 and CycK were expressed as a fusion protein with a FLAG-tag and a His-tag at the N-terminus, respectively. Sf9 cells were cultured at 27 °C for 72 h post infection. The cells were harvested by centrifugation and stored at −80 °C until use. The frozen Sf9 cells expressing FLAG-tagged hCDK12 and His-tagged hCycK were suspended in lysis buffer (50 mM Tris (pH 8.0), 300 mM NaCl, 10% (v/v) glycerol, 0.05% Brij-35, 1 mM dithiothreitol (DTT), 5 U/mL benzonase) and centrifuged at 14,000 × *g* for 30 min. The supernatant was mixed with) 10 mL pre-equilibrated FLAG resin (MBL) for 2 h with rotating at 4 °C. The FLAG resin was washed with affinity buffer (50 mM Tris (pH 8.0), 300 mM NaCl, 10% (v/v) glycerol, 0.05% Brij 35, 1 mM DTT) and eluted with 0.2 mg/mL FLAG peptide in affinity buffer. The eluate was loaded onto a HiLoad 26/60 Superdex 200 pg column (GE Healthcare) using SDX buffer (50 mM Tris (pH 8.0), 150 mM NaCl, 10% (v/v) glycerol, 0.05% Brij 35, 1 mM DTT). The purified FLAG-tagged hCDK12/His-tagged hCycK complex was concentrated with Amicon Ultra15 [MWCO:100 k] (Merck Millipore). Protein concentration was determined by using Coomassie Plus (Bradford) Assay Reagent (Thermo Scientific) with bovine serum albumin as the standard.

**Preparation of human full-length CDK13.** Human full-length CDK13 was prepared in-house with a baculovirus expression system. Human CDK13 (residues 1–1512 aa, full, Genbank Accession No. NM_003718) was co-expressed with human CycK (residues 1–580 aa, full, Genbank Accession No. NM_001099402) in Sf9 cells by using baculovirus expression system. CDK13 and CycK were expressed as a fusion protein with a FLAG-tag and a His-tag at the N-terminus, respectively. The methods for the production and purification were the same as described for FLAG-tagged hCDK12 and His-tagged hCycK proteins.

**Human CDK9, CDK12, and CDK13 enzyme inhibition assay using the LANCE system.** The inhibitory activity of the test compounds was assessed by the LANCE Ultra assay, which detects the ATP-dependent phosphorylation of an ULight-4E-BP1 (Thr37/Thr46) substrate peptide (150 nM). Briefly, the enzyme reaction was run in reaction buffer (25 mM HEPES (pH 7.5), 10 mM $MgCl_2$, 0.01% BSA, 0.01% Tween 20, 1 mM DTT). The assay was performed in 384-well plate (6 μL) format. The end concentration of the ATP substrate was 10 μM, and that of the ULight-4E-BP1 (Thr37/Thr46) substrate peptide was 150 nM. The end concentration of CDK9, CDK12 or CDK13 was 0.3 nM, 30 nM, or 30 nM, respectively. Pre-incubation of the compounds and enzyme was performed for 60 min at room temperature. After 15, 60, or 90 min incubation at room temperature, the reaction was terminated by the addition of 10 mM EDTA and 0.15 nM Eu-labeled anti-phospho-eIF4E-binding protein 1 (Thr37/46) antibody in LANCE detection buffer. Time-resolved fluorescence (excitation, 320 nm; emission donor, 615 nm; emission acceptor, 665 nm) was monitored by using an EnVision spectrophotomer (PerkinElmer). The readout was calculated as (acceptor counts/donor counts) × 1000. The $IC_{50}$ values were derived by fitting a sigmoidal dose-response curve to a plot of assay readout over inhibitor concentration. All fits were computed with the program Prism 5.03 (GraphPad Software, San Diego, CA).

**Human CDK7 and CDK8 binding assay using a Kinase Tracer.** The inhibitory activity of test compounds was assessed by using a binding assay in which Kinase Tracer 236 (an ATP competitive inhibitor) was used as a probe against GST-tagged CDK7 or GST-tagged CDK8. The bound to the CDK7 or CDK8 was detected by time-resolved fluorescence resonance energy transfer (TR-FRET) between a Europium-labelled antibody and Kinase Tracer 236; the displacement of the probe was detected by a decrease in the FRET signal. Briefly, the enzyme reaction was performed in reaction buffer (25 mM HEPES (pH 7.5), 10 mM $MgCl_2$, 0.01% BSA,

0.01% Tween 20, 2 mM DTT). The assay was performed in a 384-well plate (6 μL) format. Two microliters of different concentrations of the test compounds were added to the plate, after which 2 μL of the antibody/kinase tracer 236 mix (800-fold diluted Europium-labelled anti-GST antibody/kinase tracer 236) was added. A Kinase Tracer 236 concentration of 30 nM or 20 nM was used for CDK7 or CDK8, respectively. After the plate was incubated at room temperature for 5 min, 2 μL of 0.5 nM CDK7 or 0.2 nM CDK8 in reaction buffer was added, and the incubation was continued for a further 60 min before the plate was measured and evaluated. Time-resolved fluorescence was monitored as in the section "Human CDK12, CDK13 and CDK9 enzyme inhibition assay by using the LANCE system". The binding displacement curves were fitted to a variable-slope sigmoidal dose-response curve by using GraphPad Prism.

**Human CDK2/CCNA2 enzyme inhibition with radiometric assay.** The assays for CDK2/CCNA2 using radiolabeled [γ-$^{33}$P] ATP (GE Healthcare, Piscataway, NJ) were performed in 96-well plates. The enzyme reaction was run in reaction buffer (25 mM HEPES, pH 7.5, with 10 mM magnesium acetate, 1 mM DTT) in a total volume of 50 μL. The final concentrations of substrate Histone H1 and ATP was 1 μg/well and 500 nM, respectively. The final concentration of CDK2/CCNA2 was 1.8 mU/well. Prior to the kinase reaction, the compound and enzyme were incubated for 5 min at room temperature. The kinase reactions were initiated by the addition of ATP. After incubation for 20 min at room temperature, the reaction was terminated by the addition of 10% trichloroacetic acid (final concentration). The [γ-$^{33}$P]-phosphorylated proteins were filtered in a Harvest Plate (Millipore Corp.) with a Cell Harvester (PerkinElmer) and then free [γ-$^{33}$P] ATP was washed out with 3% phosphoric acid. The plates were dried and 40 μL of MicroScint0 (PerkinElmer) was added. The radioactivity was counted by a TopCount scintillation counter (PerkinElmer).

**Cellular HTRF CTD pSer2 detection assay in human breast cancer SK-BR-3 cells.** Human breast cancer SK-BR-3 cells were maintained in RPMI 1640 supplemented with 10% fetal bovine serum (FBS) at 37°C in a humidified 5% $CO_2$ incubator. All reagents were supplied in the HTRF Phospho-RNA Pol II (Ser2) Assay System (63ADK000U, CisBio). The cells were inoculated in a 96-well plate (Coster 3585) (100,000 cells per well; 100 μL per well) or a 384-well poly-D-lysine Cellware plate (BD 356640) (5,000 cells per well; 20 μL per well) and incubated at 37 °C in a humidified 5% $CO_2$ incubator. Cells were treated with compound per well at 37 °C for 4 h in a humidified 5% $CO_2$ incubator. The cells were washed with PBS(-) and were lysed with 50 μL or 25 μL of diluted 4-fold lysis buffer contained in the Phospho-RNA Pol II (Ser2) Assay System. Lysis was conducted at room temperature for 10 min with gentle shaking. The cell lysate was transferred to a 384-well plate (16 μL per well; Greiner 784075). A 50-fold dilution of antibody detection buffer (each 2 μL) was added to the lysed cells. The plate was incubated overnight at room temperature. The plates were analyzed on an EnVision (excitation, 320 nm; emission donor, 615 nm; emission acceptor, 665 nm). The inhibition rate was calculated based on 0% control wells (DMSO-treated cell lysates) and 100% control wells (lysis buffer). The data analysis was performed with GraphPad Prism statistical analysis software using a nonlinear regression equation for a sigmoidal dose-response with a variable slope.

**Cell viability assay in human breast cancer SK-BR-3 cells.** The SK-BR-3 human breast cancer cell lines were maintained in RPMI 1640 (Thermo Fisher Scientific, Waltham, MA). The cells were purchased from American Type Culture Collection (Manassas, VA). The media were supplemented with 10% FBS (JRH), penicillin (10,000 U/mL; Thermo Fisher Scientific), and streptomycin (10,000 μg/mL; Thermo Fisher Scientific). The cells were seeded and subcultured in 100-mm diameter dishes every 3 days. The cells ($3 \times 10^3$) were seeded into 96-well plates and

incubated overnight in 50 μL of culture medium. Subsequently, 50 μL of each compound diluted in the culture medium was added to the wells. After incubation for 72 h, viability was determined by using the CellTiter-Glo Luminescent Cell Viability Assay (Promega, Madison, WI) in accordance with the manufacturer's instructions. The $GI_{50}$ values were calculated by using GraphPad Prism 5 software with a sigmoidal dose-response curve.

**Computational Chemistry**

**Molecular docking model of compound 1 with CDK12.** Modeling and docking calculations were performed by using the Schrödinger software suite (Release 2013-2). The crystal structure of the human CDK12-CycK complex (PDB ID:4CXA) includes two CDK12 molecules (chain A and chain C). Chain C was used as a template for docking because the ATP binding site was more open than chain A, in which the ATP site is occluded by the C-terminal segment.[9] The missing side chains of the crystal structure were modeled by using Prime. All water molecules were removed before docking. The compound structure was prepared for docking by using LigPrep module and docked using Glide in SP mode with torsional constraints by SMARTS patterns: [#1][N-0X3][c-0X3][n-0X2] = 0.0 and [#1][C-0X4][N-0X3][#1] = 145.8. The docked pose was then minimized using the local optimization feature using Molecular Operating Environment (MOE) 2013.08.

**Molecular docking model of compound 1 with CDK2.** The docking calculations were performed using the Schrödinger software suite (Release 2014-3). The crystal structure of human CDK2 with a diaminopyrimidine inhibitor (PDB ID:2FVD) was used. The compound structure used was the same as that used for the CDK12 docking study above and docked by using Glide in SP mode with core constraints determined by the SMARTS pattern

S(=O)(=O)N(CC1)CCC1Nc2ncccc2, which was consistent with the conformation of the diaminopyrimidine inhibitor in 2FVD. The docked pose was then minimized using the local optimization feature using MOE 2013.08.

**Molecular docking of compound 27 with CDK12.** The X-ray structure of CDK12 kinase domain in complex with **29** was used for docking studies. The ligand **27** and protein were prepared in accordance with the standard protocol using Maestro 2015-03 (Schrodinger software). Twenty docking modes were output in Glide SP mode, which were further refined using Glide XP mode. All docking calculations were performed using default settings. The obtained 20 modes were rescored by the in-house MMGBSA calculation tool based on AMBER[51] and the pose with the best score was selected as the presumed binding pose. The common partial structure of the predicted pose of **27** well overlapped with that of **29**, which supports that this docking pose is reasonable.

## ASSOCIATED CONTENT

### Supporting Information

Overlay of co-crystal structures (PDB:4NST and PDB: 6CKX), the global kinase selectivity of **2**, time dependency for CDK12 inhibition, protein expression and purification of CDK12 for crystallization, crystallographic information of CDK12 in complex with compound **29**, small molecular X-ray crystal structure analysis of **1**, **16**, **21**, **22**, **23**, **25**, **27**, and **33** (PDF)

Molecular strings for all the compounds reported in this study (CSV)

Coordinate files of the docking models (Figure 3 and Figure 9)

A coordinate file of CDK12 in complex with compound **29** (Figure 8, PDB: 6CKX)

**PDB ID Code** : 6CKX (compound **29**).

Authors will release the atomic coordinates and experimental data upon article publication.

## AUTHOR INFORMATION

### Corresponding Author

* (M.I.) phone: +81-466-32-1196, E-mail: masahiro.ito@takeda.com; (Y.I.) phone: +81-466-32-4112, E-Mail: yasuhiro.imaeda@takeda.com

### Present Addresses

[⊥]T. Tanaka, H. Kokubo, M. Kondo, T. Kawamoto, and H. Maezaki: Axcelead Drug Discovery Partners Inc., Fujisawa-shi, Kanagawa, 251-8585, Japan.

[#]Academic Research and Industrial Collaboration Management Office, Kyushu University, 3-8-34 Momochihama Sawara-ku Fukuoka, 814-0001, Japan.

### Notes

The authors declare no competing financial interest.

### Acknowledgement

We thank Yasumi Kumagai and Motoo Iida for their assistance with NMR spectroscopic experiments and analysis, Mitsuyoshi Nishitani and Yoichi Nagano for acquiring and determining X-ray crystal structures, Yumi Imai and Haruyuki Nishida for supervising of structure determination and introduction of the CSD. We also thank Kouichi Iwanaga and Izumi Nomura for conducting high-throughput synthesis. We thank Taisuke Tawaraishi, Yoshihisa Nakada, Nobuki Sakauchi, Ryosuke Tokunoh, Keiji Kamiyama, Akihiro Yokota, Nobuo Cho, and Osamu Uchikawa for their cooperation in helping us execute this work. We thank Bi-Ching Sang and Irena Levin for the constructs encoding CDK12/CycK and CAK1p; Steve Ding for

assistance with protein purification and crystallization. We thank Jerry Tien and Grace Cheng with assistance with CDK12 biochemistry. We thank Gyorgy Snell and Wes Lane for diffraction data collection and processing, and the staff of the Berkeley Center for Structural Biology (BCSB), who operate ALS beamline 5.0.3. The BCSB is supported in part by the US National Institutes of Health, US National Institute of General Medical Sciences. The Advanced Light Source is supported by the Director, Office of Science, Office of Basic Energy Sciences of the U.S. Department of Energy under Contract No. DE-AC02-05CH11231.

**Abbreviations**

AcOK, potassium acetate; $AcONH_4$, ammonium acetate; *tert*-BuONa, sodium *tert*-butoxide; $CDCl_3$, deuterated chloroform; CCNA2, cyclin A2; CycC, cyclin C; CycH, cyclin H; CycK, cyclin K; CycT1, cyclin T1; Davephos: 2-dicyclohexylphosphino-2'-(*N,N*-dimethylamino)biphenyl; DIPEA: *N,N*-diisopropylethylamine; DMSO-$d_6$, deuterated dimethyl sulfoxide; DYRK2, dual specificity tyrosine phosphorylation regulated kinase 2; 4E-BP1, eukaryotic translation initiation factor 4E binding protein 1; eIF4E, eukaryotic initiation factor 4E; EtOH, ethanol; $Et_3N$: triethylamine; FBS, fetal bovine serum; FRET, fluorescence energy transfer; HEPES, 4-(2-hydroxyethyl)-1-piperazineethanesulfonic acid; HTRF, homogeneous time resolved fluorescence; LANCE, lanthanide chelate excitation; logD, distribution coefficient; MAT1, ménage a trois; MeCN, acetonitrile; MeOH, methanol; MMGBSA, molecular mechanics generalized born surface area; ODS, octadecyl silica; $Pd(dppf)Cl_2$, [1,1′-bis(diphenylphosphino)ferrocene]dichloropalladium(II); $Pd(dppf)Cl_2{\cdot}CH_2Cl_2$, [1,1′-bis(diphenylphosphino)ferrocene]dichloropalladium(II) dichloromethane adduct; $Pd_2(dba)_3$, tris(dibenzylideneacetone)dipalladium(0); $PdCl_2(Amphos)_2$: bis(di-*tert*-butyl(4-dimethylaminophenyl)phosphine)dichloropalladium(II);

RPMI 1640, Roswell park memorial institute medium 1640; Sf9, Spodoptera frugiperda clone 9; SMARTS, SMILES (simplified molecular input line entry specification) arbitrary target specification; STK39, serine threonine kinase 39; TAOK1, thousand and one amino acid protein kinase 1; TR-FRET, time-resolved fluorescence energy transfer; Xantphos, 4,5-bis(diphenylphosphino)-9,9-dimethylxanthene.

**References**

1. Harlen, K. M.; Churchman, L. S. The code and beyond: transcription regulation by the RNA polymerase II carboxy-terminal domain. *Nat. Rev. Mol. Cell Biol.* **2017**, *18*, 263–273.

2. West, M. L.; Corden, J. L. Construction and analysis of yeast RNA polymerase II CTD deletion and substitution mutations. *Genetics* **1995**, *140*, 1223–1233.

3. Bartolomei, M. S.; Halden, N. F.; Cullen, C. R.; Corden, J. L. Genetic analysis of the repetitive carboxyl-terminal domain of the largest subunit of mouse RNA polymerase II. *Mol. Cell. Biol.* **1988**, *8*, 330–339.

4. Heidemann, M.; Hintermair, C.; Voß, K.; Eick, D. Dynamic phosphorylation patterns of RNA polymerase II CTD during transcription. *BBA-Gene Regul. Mech.* **2013**, *1829*, 55–62.

5. Schüller, R.; Forné, I.; Straub, T.; Schreieck, A.; Texier, Y.; Shah, N.; Decker, T.-M.; Cramer, P.; Imhof, A.; Eick, D. Heptad-specific phosphorylation of RNA polymerase II CTD. *Mol*. *Cell* **2016**, *61*, 305–314.

6. Bowman, E. A.; Kelly, W. G. RNA Polymerase II transcription elongation and Pol II CTD Ser2 phosphorylation. *Nucleus* **2014**, *5*, 224–236.

7. Liang, K.; Gao, X.; Gilmore, J. M.; Florens, L.; Washburn, M. P.; Smith, E.; Shilatifard, A. Characterization of human cyclin-dependent kinase 12 (CDK12) and CDK13 complexes in

C-terminal domain phosphorylation, gene transcription, and RNA processing. *Mol. Cell. Biol.* **2015**, *35*, 928–938.

8. Kohoutek, J.; Blazek, D. Cyclin K goes with Cdk12 and Cdk13. *Cell Div.* **2012**, *7*, 12.

9. Dixon-Clarke, S. E.; Elkins, J. M.; Cheng, S. W. G.; Morin, G. B.; Bullock, A. N. Structures of the CDK12/CycK complex with AMP-PNP reveal a flexible C-terminal kinase extension important for ATP binding. *Sci. Rep*. **2015**, *5*, 17122.

10. Bösken, C. A.; Farnung, L.; Hintermair, C.; Merzel Schachter, M.; Vogel-Bachmayr, K.; Blazek, D.; Anand, K.; Fisher, R. P.; Eick, D.; Geyer, M. The structure and substrate specificity of human Cdk12/Cyclin K. *Nat. Commun*. **201**4, *5*, 3505.

11. Greifenberg, A. K.; Hönig, D.; Pilarova, K.; Düster, R.; Bartholomeeusen, K.; Bösken, C. A.; Anand, K.; Blazek, D.; Geyer, M. Structural and functional analysis of the Cdk13/Cyclin K complex. *Cell Reports* **2016**, *14*, 320–331.

12. Baumli, S.; Hole, Alison J.; Wang, L.-Z.; Noble, M. E. M.; Endicott, Jane A. The CDK9 tail determines the reaction pathway of positive transcription elongation factor b. *Structure* **2012**, *20*, 1788–1795.

13. Baumli, S.; Lolli, G.; Lowe, E. D.; Troiani, S.; Rusconi, L.; Bullock, A. N.; Debreczeni, J. É.; Knapp, S.; Johnson, L. N. The structure of P‐TEFb (CDK9/cyclin T1), its complex with flavopiridol and regulation by phosphorylation. *EMBO J.* **2008**, *27*, 1907–1918.

14. Ko, T. K.; Kelly, E.; Pines, J. CrkRS: a novel conserved Cdc2-related protein kinase that colocalises with SC35 speckles. *J. Cell Sci.* **2001**, *114*, 2591–2603.

15. Even, Y.; Durieux, S.; Escande, M.-L.; Lozano, J. C.; Peaucellier, G.; Weil, D.; Geneviève, A.-M. CDC2L5, a Cdk-like kinase with RS domain, interacts with the

ASF/SF2-associated protein p32 and affects splicing in vivo. *J. Cell. Biochem.* **2006**, *99*, 890–904.

16. Fu, X. D. The superfamily of arginine/serine-rich splicing factors. *RNA* **1995**, *1*, 663–680.

17. Bartkowiak, B.; Greenleaf, A. L. Expression, purification, and identification of associated proteins of the full-length hCDK12/Cyclin K complex. *J. Biol. Chem.* **2015**, *290*, 1786–1795.

18. Davidson, L.; Muniz, L.; West, S., 3′ end formation of pre-mRNA and phosphorylation of Ser2 on the RNA polymerase II CTD are reciprocally coupled in human cells. *Gene. Dev.* **2014**, *28*, 342–356.

19. Eifler, T. T.; Shao, W.; Bartholomeeusen, K.; Fujinaga, K.; Jäger, S.; Johnson, J. R.; Luo, Z.; Krogan, N. J.; Peterlin, B. M. Cyclin-dependent kinase 12 increases 3′ end processing of growth factor-induced c-FOS transcripts. *Mol. Cell Biol.* **2015**, *35*, 468–478.

20. Tien, J. F.; Mazloomian, A.; Cheng, S. W. G.; Hughes, C. S.; Chow, C. C. T.; Canapi, L. T.; Oloumi, A.; Trigo-Gonzalez, G.; Bashashati, A.; Xu, J.; Chang, V. C. D.; Shah, S. P.; Aparicio, S.; Morin, G. B. CDK12 regulates alternative last exon mRNA splicing and promotes breast cancer cell invasion. *Nucleic Acids Res.* **2017**, *45*, 6698–6716.

21. Blazek, D.; Kohoutek, J.; Bartholomeeusen, K.; Johansen, E.; Hulinkova, P.; Luo, Z.; Cimermancic, P.; Ule, J.; Peterlin, B. M. The Cyclin K/Cdk12 complex maintains genomic stability via regulation of expression of DNA damage response genes. *Gene. Dev.* **2011**, *25*, 2158–2172.

22. Bajrami, I.; Frankum, J. R.; Konde, A.; Miller, R. E.; Rehman, F. L.; Brough, R.; Campbell, J.; Sims, D.; Rafiq, R.; Hooper, S.; Chen, L.; Kozarewa, I.; Assiotis, I.; Fenwick, K.;

Natrajan, R.; Lord, C. J.; Ashworth, A. Genome-wide profiling of genetic synthetic lethality identifies CDK12 as a novel determinant of PARP1/2 inhibitor sensitivity. *Cancer Res.* **2014**, *74*, 287–297.

23. Joshi, P. M.; Sutor, S. L.; Huntoon, C. J.; Karnitz, L. M., Ovarian cancer-associated mutations disable catalytic activity of CDK12, a kinase that promotes homologous recombination repair and resistance to cisplatin and poly(ADP-ribose) polymerase inhibitors. *J. Biol. Chem.* **2014**, *289*, 9247–9253.

24. Natrajan, R.; Wilkerson, P. M.; Marchiò, C.; Piscuoglio, S.; Ng, C. K. Y.; Wai, P.; Lambros, M. B.; Samartzis, E. P.; Dedes, K. J.; Frankum, J.; Bajrami, I.; Kopec, A.; Mackay, A.; A'Hern, R.; Fenwick, K.; Kozarewa, I.; Hakas, J.; Mitsopoulos, C.; Hardisson, D.; Lord, C. J.; Kumar-Sinha, C.; Ashworth, A.; Weigelt, B.; Sapino, A.; Chinnaiyan, A. M.; Maher, C. A.; Reis-Filho, J. S. Characterization of the genomic features and expressed fusion genes in micropapillary carcinomas of the breast. *J. Pathol.* **2014**, *232*, 553–565.

25. Paculová, H.; Kohoutek, J., The emerging roles of CDK12 in tumorigenesis. *Cell Div.* **2017**, *12*, 7.

26. Chilà, R.; Guffanti, F.; Damia, G. Role and therapeutic potential of CDK12 in human cancers. *Cancer Treat. Rev.* **2016**, *50*, 83–88.

27. Chan, D. A.; Giaccia, A. J. Harnessing synthetic lethal interactions in anticancer drug discovery. *Nat. Rev. Drug Discov.* **2011**, *10*, 351–364.

28. Lim, S.; Kaldis, P. Cdks, cyclins and CKIs: roles beyond cell cycle regulation. *Development* **2013**, *140*, 3079–3093.

29. Brameld, K. A.; Kuhn, B.; Reuter, D. C.; Stahl, M. Small molecule conformational preferences derived from crystal structure data. A medicinal chemistry focused analysis. *J. Chem. Inf. Model.* **2008**, *48*, 1–24.

30. Schärfer, C.; Schulz-Gasch, T.; Ehrlich, H.-C.; Guba, W.; Rarey, M.; Stahl, M. Torsion angle preferences in druglike chemical space: A comprehensive guide. *J. Med. Chem.* **2013**, *56*, 2016–2028.

31. Zhang, T.; Kwiatkowski, N.; Olson, C. M.; Dixon-Clarke, S. E.; Abraham, B. J.; Greifenberg, A. K.; Ficarro, S. B.; Elkins, J. M.; Liang, Y.; Hannett, N. M.; Manz, T.; Hao, M.; Bartkowiak, B.; Greenleaf, A. L.; Marto, J. A.; Geyer, M.; Bullock, A. N.; Young, R. A.; Gray, N. S. Covalent targeting of remote cysteine residues to develop CDK12 and CDK13 inhibitors. *Nat. Chem. Biol.* **2016**, *12*, 876–884.

32. Johannes, J.; Denz, C. R.; Su, N.; Wu, A.; Impastato, A. C.; Mlynarski, S.; Varnes, J. G.; Prince, D. B.; Cidado, J.; Gao, N.; Haddrick, M.; Jones, N. H.; Li, S.; Li, X.; Liu, Y.; Nguyen, T. B.; O'Connell, N.; Rivers, E.; Robbins, D. W.; Tomlinson, R.; Yao, T.; Ferguson, A. D.; Lamb, M. L.; Manchester, J. I.; Guichard, S. Structure based sesign of aelective non-covalent CDK12 inhibitors. *ChemMedChem* **2017**, ASAP, doi: 10.1002/cmdc.201700695.

33. Bunnage, M. E.; Chekler, E. L. P.; Jones, L. H. Target validation using chemical probes. *Nat. Chem. Biol.* **2013**, *9*, 195–199.

34. Weiss, W. A.; Taylor, S. S.; Shokat, K. M. Recognizing and exploiting differences between RNAi and small-molecule inhibitors. *Nat. Chem. Biol.* **2007**, *3*, 739–744.

35. Guram, A. S.; King, A. O.; Allen, J. G.; Wang, X.; Schenkel, L. B.; Chan, J.; Bunel, E. E.; Faul, M. M.; Larsen, R. D.; Martinelli, M. J.; Reider, P. J. New air-stable catalysts for general

and efficient Suzuki−Miyaura cross-coupling reactions of heteroaryl chlorides. *Org. Lett.* **2006**, *8*, 1787–1789.

36. Huang, Q.; Johnson, T. W.; Bailey, S.; Brooun, A.; Bunker, K. D.; Burke, B. J.; Collins, M. R.; Cook, A. S.; Cui, J. J.; Dack, K. N.; Deal, J. G.; Deng, Y.-L.; Dinh, D.; Engstrom, L. D.; He, M.; Hoffman, J.; Hoffman, R. L.; Johnson, P. S.; Kania, R. S.; Lam, H.; Lam, J. L.; Le, P. T.; Li, Q.; Lingardo, L.; Liu, W.; Lu, M. W.; McTigue, M.; Palmer, C. L.; Richardson, P. F.; Sach, N. W.; Shen, H.; Smeal, T.; Smith, G. L.; Stewart, A. E.; Timofeevski, S.; Tsaparikos, K.; Wang, H.; Zhu, H.; Zhu, J.; Zou, H. Y.; Edwards, M. P. Design of potent and selective inhibitors to overcome clinical anaplastic lymphoma kinase mutations resistant to crizotinib. *J. Med. Chem.* **2014**, *57*, 1170–1187.

37. Osborne, J. D.; Matthews, T. P.; McHardy, T.; Proisy, N.; Cheung, K.-M. J.; Lainchbury, M.; Brown, N.; Walton, M. I.; Eve, P. D.; Boxall, K. J.; Hayes, A.; Henley, A. T.; Valenti, M. R.; De Haven Brandon, A. K.; Box, G.; Jamin, Y.; Robinson, S. P.; Westwood, I. M.; van Montfort, R. L. M.; Leonard, P. M.; Lamers, M. B. A. C.; Reader, J. C.; Aherne, G. W.; Raynaud, F. I.; Eccles, S. A.; Garrett, M. D.; Collins, I. Multiparameter lead optimization to give an oral checkpoint kinase 1 (CHK1) inhibitor clinical candidate: (R)-5-((4-((Morpholin-2-ylmethyl)amino)-5-(trifluoromethyl)pyridin-2-yl)amino)pyrazine-2-carbonitrile (CCT245737). *J. Med. Chem.* **2016**, *59*, 5221–5237.

38. Koch, P.; Laufer, S. Unexpected reaction of 2-alkylsulfanylimidazoles to imidazol-2-ones: Pyridinylimidazol-2-ones as novel potent p38α mitogen-activated protein kinase inhibitors. *J. Med. Chem.* **2010**, *53*, 4798–4802.

39. Hilpert, H.; Mauser, H.; Humm, R.; Anselm, L.; Kuehne, H.; Hartmann, G.; Gruener, S.; Banner, D. W.; Benz, J.; Gsell, B.; Kuglstatter, A.; Stihle, M.; Thoma, R.; Sanchez, R. A.; Iding,

H.; Wirz, B.; Haap, W. Identification of potent and selective cathepsin S inhibitors containing different central cyclic scaffolds. *J. Med. Chem.* **2013**, 56, 9789–9801.

40. CSD ver. 5.38 was used. Please refer to Cambridge Structural Data Center (CCDC) https://www.ccdc.cam.ac.uk/

41. Compound **29** is not only potent CDK12 inhibitor (CDK12 $IC_{50}$ = 13 nM), but also strong CDK2 inhibitor ($IC_{50}$ = 24 nM). Thus we did not pursuit of this series. In our experience, bicyclic hinge moiety tends to reduce CDK12 selectivity against other CDKs (data no shown).

42. In our chemistry program, we were able to solve only this co-crystal structure with **29** despite intensive crystallization effort for years.

43. Chu, X.-J.; DePinto, W.; Bartkovitz, D.; So, S.-S.; Vu, B. T.; Packman, K.; Lukacs, C.; Ding, Q.; Jiang, N.; Wang, K.; Goelzer, P.; Yin, X.; Smith, M. A.; Higgins, B. X.; Chen, Y.; Xiang, Q.; Moliterni, J.; Kaplan, G.; Graves, B.; Lovey, A.; Fotouhi, N. Discovery of [4-amino-2-(1-methanesulfonylpiperidin-4-ylamino)pyrimidin-5-yl](2,3-difluoro-6-methoxyphenyl)methanone (R547), a potent and selective cyclin-dependent kinase inhibitor with significant in vivo antitumor activity. *J. Med. Chem.* **2006**, *49*, 6549–6560.

44. Karaman, M. W.; Herrgard, S.; Treiber, D. K.; Gallant, P.; Atteridge, C. E.; Campbell, B. T.; Chan, K. W.; Ciceri, P.; Davis, M. I.; Edeen, P. T.; Faraoni, R.; Floyd, M.; Hunt, J. P.; Lockhart, D. J.; Milanov, Z. V.; Morrison, M. J.; Pallares, G.; Patel, H. K.; Pritchard, S.; Wodicka, L. M.; Zarrinkar, P. P. A quantitative analysis of kinase inhibitor selectivity. *Nature Biotechnol.* **2008**, *26*, 127–132.

45. Profile of each kinase was checked using the web site of National Center for Biotechnology Information (NCBI), TAOK (gene ID 57551), DYRK2 (gene ID: 8445), and STK39 (gene ID: 27347).

46. The Human Protein Atlas website (https://www.proteinatlas.org/)

47. Cho, S.-J.; Kim, Y.-J.; Surh, Y.-J.; Kim, B. M.; Lee, S.-K. Ibulocydine is a novel prodrug Cdk inhibitor that effectively induces apoptosis in hepatocellular carcinoma cells. *J. Biol. Chem.* **2011**, *286*, 19662–19671.

48. Physicochemical property of **34**, Solubility at pH 6.8 = 2.3 μg/mL, PAMPA permeability pH 7.4 = 294 nm/s, logD at pH 7.4 = 2.70.

49. Nakashima, S.; Yamamoto, K.; Arai, Y.; Ikeda, Y. Impact of physicochemical profiling for rational approach on drug discovery. *Chem. Pharm. Bull.* **2013**, *61*, 1228–1238.

50. Masumoto, K.; Takeyasu, A.; Oizumi, K.; Kobayashi, T. Studies of novel 1,4-dihydropyridine Ca antagonist CS-905. I. Measurement of partition coefficient (log P) by high performance liquid chromatography (HPLC). *Yakugaku Zasshi* **1995**, *115*, 213–220.

51. Salomon-Ferrer, R.; Case, D. A.; Walker, R. C., An overview of the Amber biomolecular simulation package. *WIREs Comput. Mol. Sci.* **2013**, *3*, 198–210.

## Table of Contents graphic